

On the geology and the geotechnical properties of pyroclastic flow deposits of the Colli Albani

Manuela Cecconi · Maurizio Scarapazzi ·
Giulia M. B. Viggiani

Received: 2 April 2009 / Accepted: 20 November 2009
© Springer-Verlag 2010

Abstract This paper presents the results of an experimental investigation into the engineering geology properties of three pyroclastic deposits from the Colli Albani volcanic complex, typical of the subsoil of Rome (Italy). In their natural state, these materials are coarse-grained weak rocks, generally unsaturated in situ. The mechanical properties of the material are related to the geological origin of the deposits, their formation environment and mechanisms. These are also revealed by peculiar micro-structural features. A technical sheet for the description and classification of these deposits is proposed in the paper. The experimental investigation consisted mainly of identification and classification tests, one-dimensional compression and direct shear tests on saturated and dry samples. Due to their nature, non standard techniques had to be developed for sample preparation and testing. The main findings on compressibility, shear strength and creep properties of the materials are presented in the paper. Special attention is given to the definition of the failure envelope at relatively low confining stress and to the assessment of the influence of saturation on shear strength parameters.

Keywords Pyroclastic deposits ·
Technical classification · Physical properties ·
Compressibility · Shear strength

Résumé L'article présente les résultats de travaux expérimentaux relatifs aux propriétés géotechniques de trois dépôts pyroclastiques issus de la formation volcanique de Colli Albani, typique du sous-sol de Rome (Italie). A l'état naturel, ces matériaux sont des roches tendres à grain grossier, généralement non saturées in situ. Les propriétés mécaniques de ces matériaux doivent être mises en rapport avec l'origine géologique des dépôts, les contextes environnementaux et les processus de formation, ces derniers étant révélés par des caractéristiques micro-structurales particulières. Une fiche technique est proposée dans l'article pour la description et la classification de ce type de dépôt. Les travaux expérimentaux ont consisté principalement en des tests d'identification et de classification, des essais de compression simple et des essais de cisaillement direct sur des échantillons saturés ou secs. Du fait de la nature de ces matériaux, des techniques particulières ont dû être mises en œuvre pour la préparation des échantillons et les essais. Les principaux résultats relatifs à la compressibilité, la résistance au cisaillement et les caractéristiques de fluage de ces matériaux sont présentés dans l'article. Une attention particulière est donnée à la définition de la courbe de rupture sous relativement faible confinement et à l'évaluation de l'influence de la saturation sur les paramètres de résistance au cisaillement.

M. Cecconi (✉)
Department of Civil and Environmental Engineering,
University of Perugia, Perugia, Italy
e-mail: ceccon@unipg.it

M. Scarapazzi
Geoplanning S.r.l., Rome, Italy

G. M. B. Viggiani
Department of Civil Engineering,
University of Roma Tor Vergata, Rome, Italy

Mots clés Dépôts pyroclastiques ·
Classification technique · Propriétés physiques ·
Compressibilité · Résistance au cisaillement

Introduction

Pyroclastic deposits cover large parts of Central and Southern Italy, totalling some 8–9,000 km². Volcanoclastic deposits of southern Italy—both airfall and flow deposits—have been extensively studied in the literature (e.g.: Croce et al. 1961; Pellegrino 1967; Evangelista and Aversa 1994; Del Prete et al. 1998; Esposito and Guadagno 1998). In central Italy, the main volcanic complexes in the area of Rome are the Monti Sabatini, 30 km to the north-west, and the Colli Albani, about 25 km to the south-east of the city. The rocks from these volcanic complexes are very significant in the development of the Rome area, creating fertile soils but also high, steep slopes which are easily quarried for building materials. Pozzolanas have been continuously exploited since Roman and Etruscan times to produce hydraulic mortars and cement; they are still often used as sub-grade for roads and tennis courts.

This study of the geotechnical properties of the “soft” pyroclastic rocks (or pozzolanas) beneath Rome was initiated some ten years ago, driven by the need to analyse the stability of sub-vertical cuts and the underground cavities frequently encountered in many parts of the city. Mining activities over the centuries have resulted in a complex network of underground cavities and in some cases sudden collapses have occurred with the formation of sinkholes at the surface (Bernabini et al. 1966; Lembo Fazio and Ribacchi 1990), but numerous underground cavities have not yet been surveyed or mapped. Open pozzolana quarries are also common in the south east of Rome, with sub-vertical excavation faces which can be as high as 20–25 m.

Cecconi (1999), Cecconi and Viggiani (2000, 2001), and Cecconi et al. (2003) describe the main outcomes of a detailed study of the mechanical properties of the Pozzolana Nera, belonging to the III cycle of the Tuscolano-Artemisia eruptive phase of the Colli Albani (De Rita 1988). Their work was based on saturated samples, but as these materials are generally above the water table and only partly saturated in situ ($S_r = 0.4/0.5$), further research and experimental work on the hydraulic and mechanical properties of the partially saturated material was carried out for both basic research and engineering applications. Some of this work was presented by Cattoni (2003) and Cattoni et al. (2007).

The present paper focuses on the results of a recent comparative geological and geotechnical investigation of two additional pyroclastic flow deposits of the Colli Albani, locally known as Pozzolanelle and Conglomerato Giallo, belonging respectively to the IV and II cycles of the Tuscolano-Artemisia eruptive phase of the Colli Albani (De Rita et al. 1988).

As pointed out by Karner et al. (2001), because of the many uses of this material over the long history of the

area, a confusing nomenclature for the rock units of the Colli Albani has built up over the years. The volcanic rocks from the Colli Albani have often been identified on the basis of the geographic location of outcrops and quarries or their colour; more rarely on the basis of their physical and mechanical properties, in part because of the difficulty of intact sampling of these materials for laboratory testing (Cecconi 1998). Often these units have been mis-identified because of similar physical characteristics and ambiguous terminology. From a strictly geological point of view, these units can be distinguished unequivocally only through geochemical or radio-isotopic analysis, as done, for example, by Karner et al. (2001). The technical description sheet proposed here is simply an aid to a standard description of pyroclastic soils and to facilitate a better qualitative and semi-quantitative assessment of some of the main properties of the material.

Measurement of the physical properties and mechanical characteristics of the two materials under investigation was intentionally carried out using common laboratory techniques, including conventional one-dimensional and uniaxial compression tests, indirect tension tests and direct shear tests. Due to the pyroclastic nature of the materials, special non-standard procedures were developed for the preparation of the natural samples, including rotary coring of frozen samples. Some of the experimental results obtained on reconstituted and natural samples of Pozzolanelle and Conglomerato Giallo are compared with those obtained in a much wider experimental programme on the Pozzolana Nera.

However, in this study, the aim was not to give average values of the mechanical properties but rather to identify some of the problems that may be encountered in the laboratory characterisation of these materials and to guide the choice of suitable testing programmes. In an attempt to relate the microscopic features and the macroscopic response of the two materials, optical and electron scanning microscopy was also undertaken.

Geological origin

The Colli Albani volcanic complex is in the southernmost part of Lazio (Central Italy). The most important structure is the central caldera (Giordano et al. 2006) which was formed about 600,000 years ago (De Rita et al. 1995). Different periods of activity have been recognised, which resulted in the deposition of 300 km³ of materials, mainly pyroclastic, which outcrop extensively to the south of the river Aniene and east of the river Tiber. The presence of magmatic and lahar deposits indicates that the volcano is still active although quiescent, with fumarole activity

(Funiciello et al. 2003). The last explosive eruption was at the time of Tullio Ostilio (673 BC–641 BC).

Despite several stages of volcanic activity, the different explosive phases are homogeneous from the geochemical point of view (Fornaseri et al. 1963; Ferrara et al. 1985; Turi et al. 1991; Serri et al. 1991) and are effectively uniform in terms of petrochemical composition (Trigila et al. 1995).

Based on research carried out over the last forty years, a number of classifications have been proposed for the products of the Colli Albani, related to the time of their origin (eruptive period, eruptive epoch, eruption and single eruptive phase; Fisher and Schmincke 1984). Fornaseri et al. (1963) and Alberti et al. (1967) identified early central activity followed by both central and effusive/explosive activity, followed in turn by a phreato-magmatic phase. De Rita et al. (1988, 1995) refers to this early period

of activity as the Tuscolano-Artemisio phase (from 0.6 to 0.3 My ago) and suggests it resulted in approximately 280 km³ of mainly pyroclastic flow deposits or ignimbrites (Fig. 1). The Cinta Tuscolano-Artemisia is the only part of the caldera structure which is visible today. The Faete phase (from 0.3 to 0.2 My ago) is related to a central strato-volcano inside the caldera while the final Hydromagmatic phase (200 to 20 My ago) resulted in <1 km³ of material from the interaction of ground water with the magma.

In recent years, a revision of the 1:50,000 geological map (CARG 1992) led to a new methodology of classification (De Rita et al. 2000; Giordano et al. 2006). The volcanic units are organised in lithosomes recognised by their typical morphologies (Salvador 1987). Table 1 shows a comparison of the different classification systems for the Colli Albani. According to Giordano et al. (2006), the Pozzolanelle is present at the lower limit of the

Fig. 1 Geological map of the Colli Albani volcanic complex (Giordano et al. 2006)

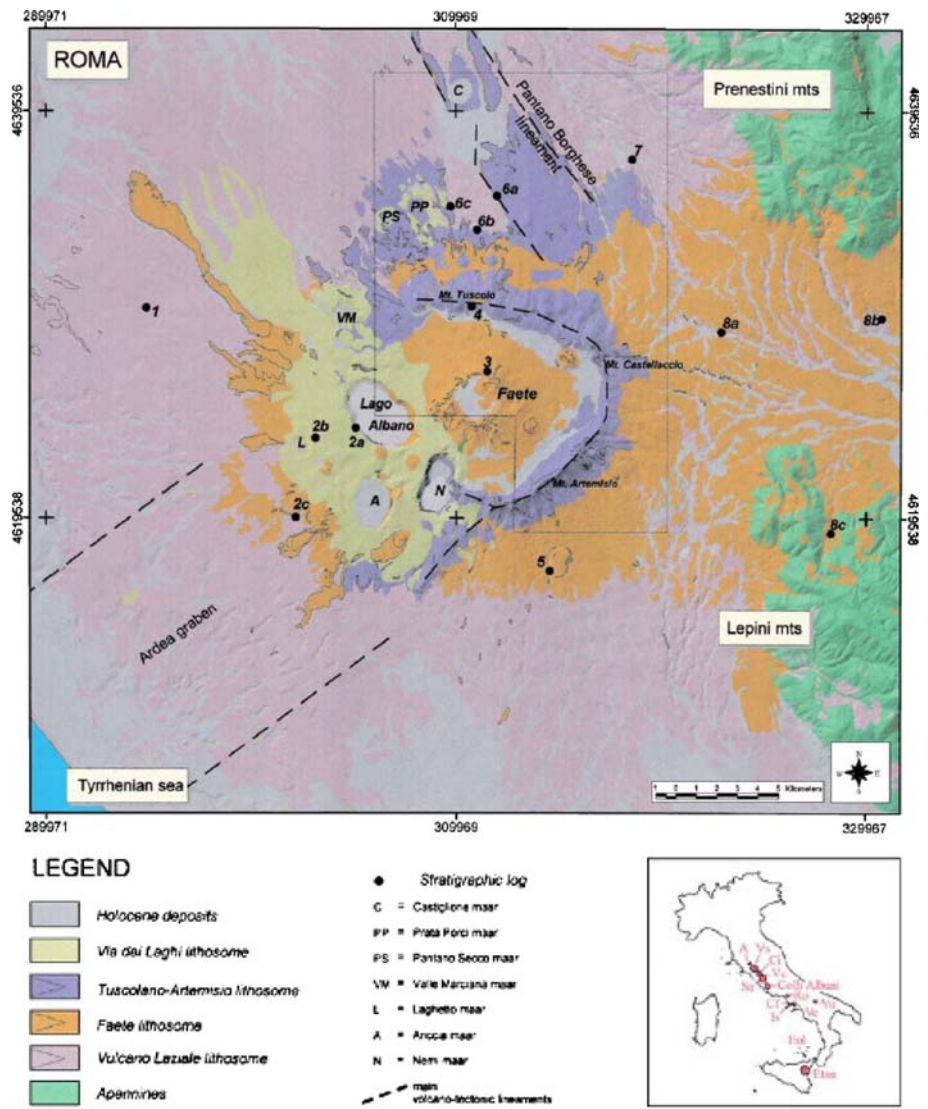



Table 1 Colli Albani volcanic complex

Alberti et al., 1967	Fornaseri et al., 1963	De Rita et al., 1988	Giordano et al., 2005	Formations analysed in this paper
Final eruptive episodes	External vents phreatomagmatic activity	Hydromagmatic final Phase	Via dei Laghi Lithosome	
External eruptive apparatus	Final activity of the main crater	Faete Phase	Faete Lithosome	
Central eruptive apparatus	Products of the TA activity	Tuscolano-Artemisia Phase	Tuscolano Artemisio Lithosome	
	Inferior Tuffs Complex		Vulcano Laziale Lithosome	
	Vulcano Laziale early products			

Comparison between stratigraphical denominations proposed by different authors with indication of investigated formations (adapted from Giordano et al. 2006)

Tuscolano-Artemisio lithosome (De Rita et al. 1988), while the Pozzolana Nera and the Conglomerato Giallo can be ascribed to the Vulcano Laziale lithosome.

At the macro-scale, Pozzolanelle is massive and chaotic. Diano (2005) defined four different facies of the eruption unit, the fourth of which, forming the top unit of the Tuscolano-Artemisio lithosome, is mainly dark grey to dark red/brown, ashy, and reaches a maximum thickness of about 4 m. The composition is tephritic-phonolitic (Freda et al. 1997; Gaeta et al. 2006).

The Pozzolanelle is uncemented and although the lower portion can occasionally be lithified, generally it presents transitional features with the Tufo Lionato, also belonging to the Villa Senni eruption unit. This material is lithoidal with an extensively zeolitised matrix rich of chabasite and phillipsite. Underlying the Tufo Lionato is the deposit Pozzolana Nera which consists of a thin level of fallout materials (scoriaceous lapilli with lithic fragments and crystals of leucite and pyroxene) at the bottom of an ashy level about 0.3 m thick. In its central portion, the deposit is massive and chaotic, mainly formed by ignimbrites. Its maximum thickness is approximately 20 m. The matrix consists mostly of dark grey to black fine ash shards, and crystals such as leucite, clinopyroxene and biotite (Giordano et al. 2006).

The Conglomerato Giallo is a succession of pyroclastic deposits with particle sizes ranging from ash to lapilli. It consists primarily of rounded altered yellow and red

scorias with secondary volcanic lithics and clinopyroxene, biotite and altered leucite crystals (mm to cm in size). This deposit varies in grading and forms in somewhat chaotic banks or lenses which vary in thickness from 2–3 m to a maximum of about 20 m in the area of the Basilica of S. Paolo fuori le Mura. Both the geometry and the dominance of the juvenile/scoriaceous component suggest a syn-eruptive origin, probably linked to remoulding of the scoria cones formed along peri-calderic fractures following the eruption of the Pozzolane Rosse. The most likely depositional mechanism is debris flow or hyperconcentrated flow inside a wide depression at the top of the Pozzolane Rosse in the north western sector of the Colli Albani volcanic complex.

All three deposits can be clearly identified in Fig. 2, which shows a sub-vertical cut in a quarry in via di Fioranello, south east of Rome.

Technical classification of pyroclastic soils

The geological complexity of pyroclastic rocks/soils makes it difficult to classify these deposits using conventional systems. The heterogeneity of the soil mass depends on several factors, such as viscosity, temperature, chemical interaction, eruption energy, distance from the magma chamber, etc. These factors may differ within the same depositional flow and they generally vary due to the



Fig. 2 Sub-vertical cut in a quarry of Pozzolana; from the bottom it is possible to recognise the layers of Pozzolana Nera ($\cong 10$ m), Tufo Lionato ($\cong 5$ m), and Pozzolanelle ($\cong 8$ m)

interaction between the pyroclastic flow, the pre-existent morphology and the ground water. Further complexities may be induced by post-depositional processes such as welding, cementation, fissuring and chemical weathering.

For these materials, therefore, the geological and geo-technical classification systems commonly used for the majority of natural soils—probably less problematic than volcanic soils—may be inadequate or just incomplete. For this reason an original descriptive model for volcanic soils has been developed, applying some of the specific terminology of volcanology (Scandone and Giacomelli 1998).

The technical classification is based on an operationally tested data sheet, shown in Fig. 3, which can be compiled in situ for each eruptive unit observed on outcropping formations, exposed in artificial cuts, or on cores obtained by sampling as well as on retrieved samples in the laboratory. The data sheet serves the double purpose of providing an index to follow for the standard description of pyroclastic soils and a working tool to define qualitatively and semi-quantitatively some preliminary properties of the material, taking into account also the results of in situ or laboratory tests, if any. Field annotations can also be very useful in order to plan any subsequent experimental investigation.

Items 1–4 in Fig. 3 are self-explanatory and provide the basic information needed for future reference.

Item 5—pyroclastic type. In this paper, the term “pyroclastic soil/rock” refers to soil/rock consisting of more than 75% of fragments originating from volcanic activity (Gillespie and Styles 1999). The following aspects are considered:

(a) *Lithoid or semi-lithoid*: the pyroclasts (the clasts composing the pyroclastic rock) are strongly welded together and the deposit behaves as a soft rock. This

SITE:.....		OPERATOR:.....		DATE:.....	
1. STATION:.....		2. LAYER:.....		3. THICKNESS:.....	
4. ORIENTATION:.....					
5. PYROCLASTIC TYPE					
<input type="checkbox"/> Lithoid <input type="checkbox"/> Welded <input type="checkbox"/> Granular <input type="checkbox"/> Altered <input type="checkbox"/> Deeply altered					
6. COLOUR					
		Matrix		Munsell code	
		dry			
		wet		Munsell code	
		Clasts		Munsell code	
		dry			
		wet		Munsell code	
7. SEDIMENTARY STRUCTURE					
<input type="checkbox"/> Stratified..... <input type="checkbox"/> Graded..... <input type="checkbox"/> Laminated..... <input type="checkbox"/> Massive..... <input type="checkbox"/> Homogeneous..... <input type="checkbox"/> Not homogeneous.....					
8. CLAST NATURE					
<input type="checkbox"/> % Juvenile		<input type="checkbox"/> % Matrix			
<input type="checkbox"/> % Secondary		<input type="checkbox"/> % Clasts = <input type="checkbox"/> % Scoria + <input type="checkbox"/> % Pumices + <input type="checkbox"/> % Crystals			
<input type="checkbox"/> % Other (accidental sedimentary/ xenolites / sedimentary)					
9. TEXTURE					
<input type="checkbox"/> Granular sustained <input type="checkbox"/> Intermediate <input type="checkbox"/> Matrix sustained					
10. CLAST ORIENTATION					
<input type="checkbox"/> Isotropic <input type="checkbox"/> Anisotropic <input type="checkbox"/> Imbricated (Attitude).....					
11. GRADING					
Blocks / Bombs (> 64mm) <input type="checkbox"/>		Lapillus (2 - 64mm) <input type="checkbox"/>		Coarse ash (0.063 - 2 mm) <input type="checkbox"/>	
				Medium to Fine ash (< 0.063 mm) <input type="checkbox"/>	
12. ANGULARITY					
<input type="checkbox"/> Very angular <input type="checkbox"/> Angular <input type="checkbox"/> Subangular <input type="checkbox"/> Subrounded <input type="checkbox"/> Rounded <input type="checkbox"/> Very rounded					
13. VESICULATION					
<input type="checkbox"/> High <input type="checkbox"/> Medium <input type="checkbox"/> Low <input type="checkbox"/> Absent					
14. POROSITY					
<input type="checkbox"/> High <input type="checkbox"/> Medium <input type="checkbox"/> Low					
15. BONDING					
<input type="checkbox"/> True		<input type="checkbox"/> Electrostatic			
<input type="checkbox"/> Apparent		<input type="checkbox"/> Welding		<input type="checkbox"/> Low	
<input type="checkbox"/> Absent				<input type="checkbox"/> Medium	
				<input type="checkbox"/> High	
NOTES:					

Fig. 3 Data sheet for the technical classification of pyroclastic soil/rock

type of deposit is often represented by zeolitized or variously cemented tuffs.

- (b) *Welded*: the pyroclasts are held together even without capillary tension. This soil often has an intermediate behaviour between welded granular soils and soft rocks (pyroclastic flow deposits usually belong to this class).
- (c) *Granular*: the pyroclasts are not linked one to each other even if apparent cohesion may be present. These deposits behave as loose granular soils. Pyroclastic fall deposits may sometimes belong to this class.
- (d) *Altered*: directly deriving from the former classes, it is deeply modified by an alteration process which has partly destroyed the original structure. These materials usually have an intermediate behaviour between fine grained soils and granular soils.
- (e) *Deeply altered*: the product of an alteration process which has completely destroyed the original structure of the volcanic rock. These materials behave as fine grained soils.

Item 6—colour: The colour may give qualitative information on the mineralogical composition of the single pyroclast or of the whole deposit. Colour is defined both for the matrix and the clasts. Tone indicates if the colour is dark or light and gives qualitative and indirect information on the saturation degree, e.g. black to dark green is typical of material containing iron and magnesium or the presence of organic components; red indicates oxidized iron and green reduced iron. It is recommended that the colour is determined on both dry and saturated material to obtain the relation between chromatic variation and saturation degree; natural saturation conditions may also be recorded. If considered useful, the colour of the individual pyroclasts may be indicated in the Notes, i.e.: colour of scorias, colour of crystals etc. The chromatic aspect of the soil can be referred to the Munsell Colour Chart code (Hue, Value and Chroma).

Item 7—sedimentary structure: In this context, structure refers to the layer under examination, considered as a lithotechnical unit. By tradition, it is referred to as stratified (thickness >10 mm), laminated (thickness <10 mm), graded or massive. If only one horizon is present, the term stratified is not relevant. If gradation is present it is better to refer to one of the terms given in Fig. 4. If a trend is identified (flat and parallel, crossed or lenticular), this should be recorded in the Notes. The data sheet should also note whether the material is homogenous or inhomogeneous.

Item 8—clast nature: gives the percentage of the clasts with a particular origin:

- (a) juvenile (produced directly from cooling magma during transport prior to primary deposition). The

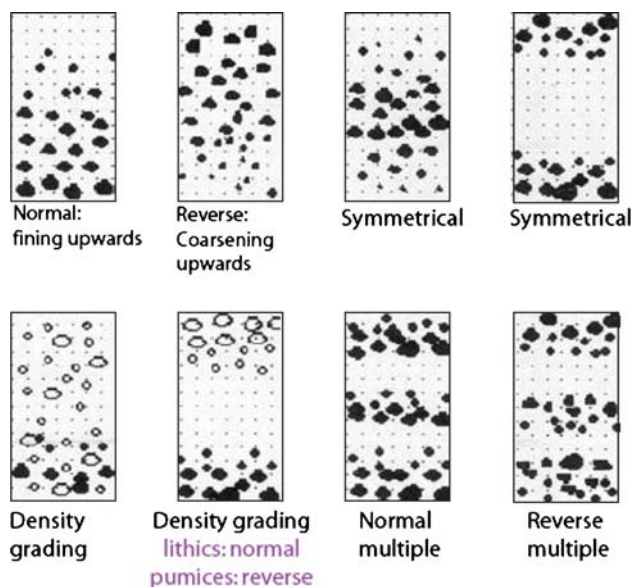


Fig. 4 Terminology for gradation (Scandone and Giacomelli 1998)

- juvenile component can also be divided into scoria, pumices and crystals;
- (b) secondary or cognate (formed during earlier volcanic activity, but which have been detached and ejected with other pyroclastic debris during a later eruption);
- (c) accidental (generated by disruption as a direct result of volcanic action, but not formed by previous activity of the volcano, generally belonging to the sedimentary basement: xenolites, mantle fragments, sedimentary).

The mineralogical nature of the components may be described in the Notes on the basis of macroscopical characteristics but further analysis (thin section, diffractometry, microprobe) may be required.

Item 9—texture: describes the relation between the clasts and the fine matrix (volcanic ash), using the following terms:

- (a) granular sustained: closed texture with interlocked clasts;
- (b) intermediate: either frequent contacts without locking or occasional contact points between clasts;
- (c) matrix sustained: coarse fraction dispersed in a prevalent matrix.

Item 10—clast orientation: the orientation of the volcanic particles can occur both during and after deposition. The following situations can be identified:

- (a) isotropic: elongated or flat clasts do not have a particular direction but are randomly oriented and dispersed;
- (b) anisotropic: elongate or flat clasts have the same orientation, which is parallel to the layer. In this case the declination should be recorded;
- (c) imbricated: elongated or flat clasts have the same orientation which is different from the declination of the layer; again the declinations of the clasts should be determined;

Item 11—Grading: determines the percentage of clasts of various sizes: blocks or bombs ($d > 64$ mm), lapillus ($2 < d < 64$ mm), coarse ash ($0.063 < d < 2$ mm), medium to fine ash ($d < 0.063$ mm).

The above classification has been modified from that originally proposed by Fischer and Schminke (1984) so that the conventional boundary between lapillus and ash corresponds to a standard sieve size. After grading, the pyroclastic rock can be classified following Gillespie and Styles (1999); see Fig. 5. In the Notes, each fraction can be further subdivided based on the particle nature, usually for the coarser fraction as ashes can be defined only by microscopic analyses.

Item 12—angularity: the degree of angularity can be analytically determined (Miura et al. 1997) or by visual

Fig. 5 Classification for **a** pyroclastic rocks and **b** pyroclastic sediments (Gillespie and Styles 1999)

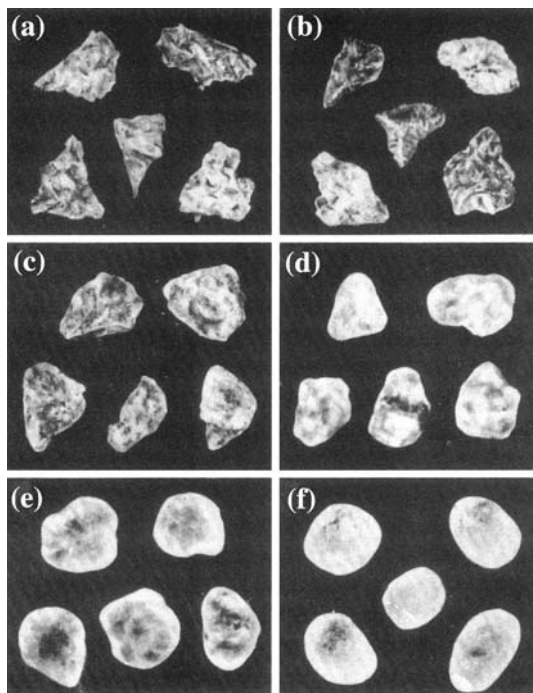
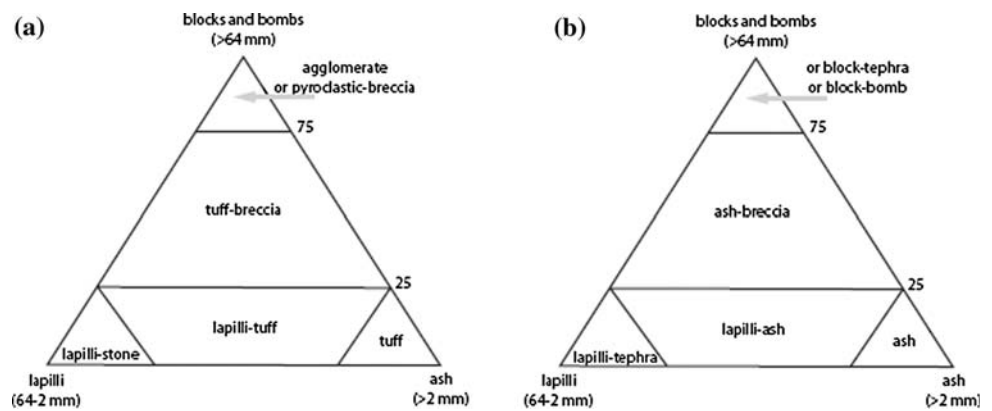


Fig. 6 Degree of angularity: **a** highly angular, **b** angular, **c** subangular; **d** subrounded; **e** rounded; **f** highly rounded. (Powers 1953, modified by Shepard 1963)

comparison with tables of standard profiles, see Fig. 6 (Powers 1953, modified by Shepard 1963). Clasts can thus be divided into 6 classes: very angular, angular, subangular, subrounded, rounded, and very rounded.

Item 13—vesiculation: describes the presence of more or less developed “bubble holes”, created by gases during the fragmentation process; in an explosive eruption the sudden decrease of pressure inside the vent causes the gas to expand and as a consequence, magma fragmentation. The degree of vesiculation can be referred to the single particle (scoria or pumices) or to the whole deposit. Vesiculation can be defined qualitatively as absent, low,

medium or high. A quantitative definition is also possible by weighing the entire particle first and then the crushed particle. The vesiculation index, $V(\%)$, can be determined as:

$$V(\%) = 100 \times \frac{ERD - CD}{ERD}$$

where ERD is the Equivalent Rock Density or the crushed material density, while CD is the Clast Density. With reference to the single particle, Houghton and Wilson (1989) suggest the following classification: 0–5% not vesiculated; 5–20% incipient vesiculation; 20–40% little vesiculation; 40–60% medium vesiculation; 60–80% highly vesiculated; >80% extremely vesiculated.

Item 14—porosity: the porosity of the material can be defined qualitatively as low, medium or high and quantitatively by the calculation of voids ratio (which should be recorded in the Notes). However, the voids ratio calculation does not take the clasts’ internal voids into account. In the case of welded deposits, but also in general, this aspect cannot easily be defined in the preliminary phases.

Item 15—bonding: may be either true (cannot be degraded by water saturation) or apparent (deriving from the suction in partly saturated soils). Small interparticle forces of an electrostatic nature may exist in the clays deriving from the alteration of pyroclastic rocks. True welding is related to syn- and post-depositional processes (cooling, chemical cementation by mineral, zeolites etc) and can be high, medium or low. Apparent bonding can be quantitatively defined as the difference between the cohesion of the soil at the natural water content and that of the same soil in saturated conditions. Apparent and true bonding may coexist.

The technical classification method described above was tested for the three pyroclastic deposits under examination. The examples given in the Appendix are from samples collected from a quarry some 10 km south of Rome.

Pozzolanelle

The classification exercise indicates that Pozzolanelle are a welded pyroclastic rock with light reddish brown clasts in a pinkish white matrix when dry and reddish brown clasts in a pinkish grey matrix when wet. Their structure is massive and quite homogeneous at the scale of the deposit, presenting limited local variations in grading. However, there was a 1 m thick horizon with a significant increase of the cinder fraction near the top of the deposit which was not considered in the description.

The pyroclasts are more than 90% juvenile, with 60% matrix and 30% clasts (20% scoria, 5% pumices and 5% crystals). The texture is intermediate with few contacts between randomly oriented clasts (isotropic).

The material falls in the lapilli-tuff field of Fischer's chart, consisting of lapilli (50%) coarse ashes (40%) and medium to fine ashes (10%), while blocks and bombs are totally absent. Clast shape is sub angular; vesiculation is low to absent.

Porosity is medium to high: laboratory determination of voids ratio yielded a value of $n = 0.64 \pm 0.01$. True bonding is medium and related to the formation of secondary minerals; apparent cohesion is revealed by shear tests carried out in dry and saturated conditions.

Pozzolana Nera

Pozzolana Nera is a welded pyroclastic rock with light grey clasts in a greenish grey matrix when dry, or dark greenish grey matrix when wet. Its structure is massive and relatively homogeneous at the scale of the deposit, presenting only limited local variations in grading.

The pyroclasts, in all size classes, are mainly juvenile (95%), with 65% matrix and 35% (30% scoria clasts, no pumice) and 5% crystals. The texture of the material is intermediate between granular- and matrix-sustained with randomly oriented clasts (isotropic).

The material consists of lapilli (>50%), coarse ashes (30%) and medium to fine ashes (<20%) while blocks and bombs are totally absent. Clast shape varies from sub-angular to angular, although clast agglomeration tends to increase the angularity. Vesiculation is low to absent.

Porosity is medium to low: laboratory determination of voids ratio yielded a value of $n = 0.45 \pm 0.01$. True bonding is medium to high, probably due to the mechanism of deposition rather than diagenetic factors.

Conglomerato Giallo

Conglomerato Giallo is a lithoid pyroclastic rock with clasts of various colours (dark bluish grey, pinkish brown, black) in a light yellowish brown matrix when dry and

brown matrix, when wet. Its structure is massive and quite homogeneous at the scale of the deposit.

The pyroclasts are 80% juvenile, with 50% matrix and 30% clasts, of which 20% are scoria, 5% pumices, and 5% crystals, 15% secondary, with only 5% rock fragments of volcanic origin or accidental. The texture is matrix sustained.

The material falls in the lapilli-tuff field of Fischer's chart, consisting of lapilli (30%), coarse ashes (35%), and medium to fine ashes (35%); blocks and bombs are totally absent. Clast shape is sub angular; vesiculation is low to absent.

Porosity is low: laboratory determination of voids ratio yielded a value of $n = 0.29 \pm 0.01$. True bonding is high, associated with diagenetic factors.

Microstructural features and physical properties

Published data (Cecconi and Viggiani 2001) on thin sections of Pozzolana Nera in plane-polarised light show that the material has a clastic texture, diffused in a scoriaceous matrix containing frequent crystals of leucite, pyroxene and biotite as well as lithic fragments of lava. Scanning electron microscopy (SEM) of a small titanium-coated dried sample of Pozzolana Nera also shows that the microstructure of the material consists of sub-angular grains of very variable size with a rough and pitted surface, at times bonded by physical bridges of the same mineralogical nature as the grains, and evenly coated by microspherules with a minimum diameter of about 0.5 μm .

As part of this study, the structural features, mineralogical composition and texture of the other two deposits under investigation were also examined by means of optical and electronic microscopy. Figures 7 and 8 show thin sections (30 μm) of Pozzolanelle and Conglomerato

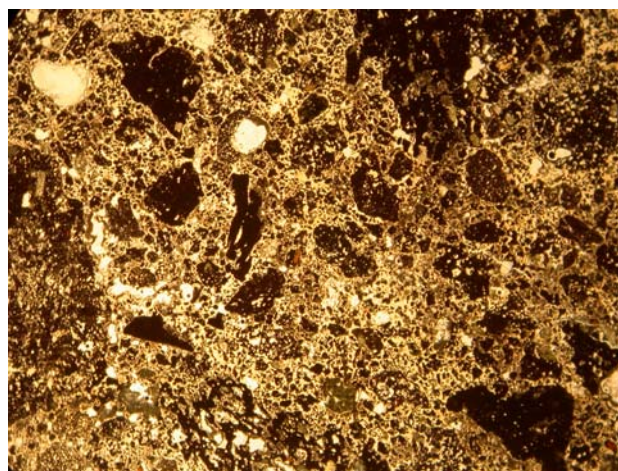


Fig. 7 Thin section (30 μm) of Pozzolanelle

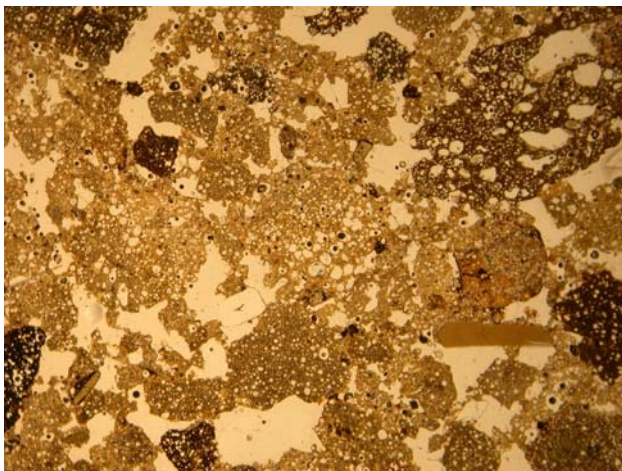


Fig. 8 Thin section (30 μm) of Conglomerato Giallo

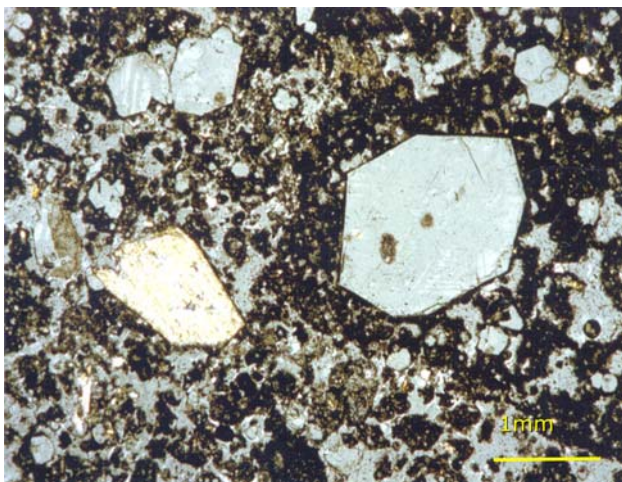


Fig. 9 Thin section (30 μm) of Pozzolana Nera in plane polarised light

Giallo respectively; for comparison, Fig. 9 shows a published thin section of Pozzolana Nera in plane-polarised light.

In thin section, the Pozzolanelle appear to consist of a compact matrix containing darker clasts, scoria with various degrees of vesiculation and frequent crystals, recognizable from their straight edges. The Conglomerato Giallo has a better defined clastic texture, diffused in a yellowish brown scoriaceous matrix containing frequent crystals as well as lithic fragments of lava, probably derived from the volcanic chimney. The mineralogical nature of the crystals would have been better defined in plane polarised light but is likely to consist mainly of leucite, biotite and clinopyroxene. In thin section, pores appear as white areas with no defined edges. Inter-granular pore features, such as size, shape, and orientation are very variable, particularly in the case of the Conglomerato Giallo; for both materials, inter-granular

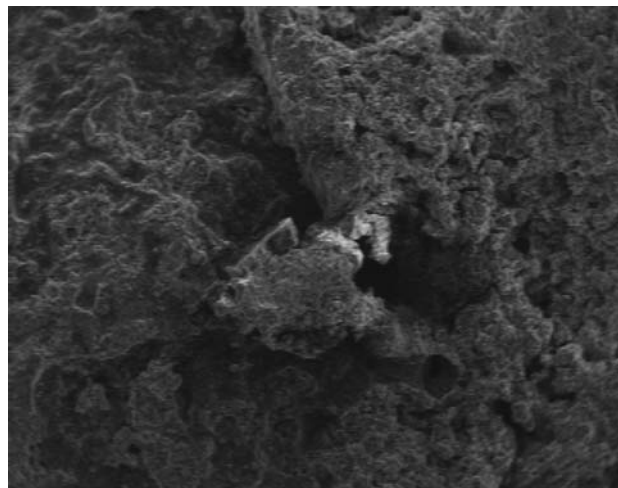


Fig. 10 SEM Pozzolanelle MF 30X

pores appear to be partially filled by altered material and secondary minerals. Intra-granular pores are generally isometric. The closed porosity, within the clasts, is very small, as confirmed by measurements of specific gravity carried out on increasingly finer, powdered material.

SEM of small samples ($\cong 1 \text{ cm}^3$) of Pozzolanelle and Conglomerato Giallo was carried out without spattering, as both materials showed no significant tendency to become electrically charged, at least for the typical duration of the observations. At a magnification of $30\times$ (Fig. 10) the scoriaceous matrix of Pozzolanelle can be observed, while it is difficult to recognise individual clasts. At larger magnifications Fig. 11a and b, it is possible to recognise secondary minerals (zeolites) growing in the pores. This indicates the bonding is partly diagenetic, i.e. chemical alteration of the constituent minerals, leading to lithification by formation of hydrated aluminosilicates (zeolites).

Figure 12a shows the clastic texture of the Conglomerato Giallo as observed by SEM at a magnification factor of 40. Again it is possible to recognize secondary minerals growing in the pores (Fig. 12b at a magnification factor of 1530).

At the scale of the laboratory sample, all three materials are quite heterogeneous. Values of average physical properties are summarised in Table 2. The grain size distribution depends strongly on the techniques adopted to separate larger aggregates before sieving and on the methods and time employed for sieving (see Camponeschi et al. 1982; O'Rourke and Crespo 1988; Lee 1991). Two different techniques were adopted to prepare the samples. The first procedure, originally developed for the Pozzolana Nera (Cecconi and Viggiani 1998), consists of breaking the material by hand while immersed in water with a detergent additive to allow separation of small aggregates. Alternatively, the material was broken by cycles of freezing and

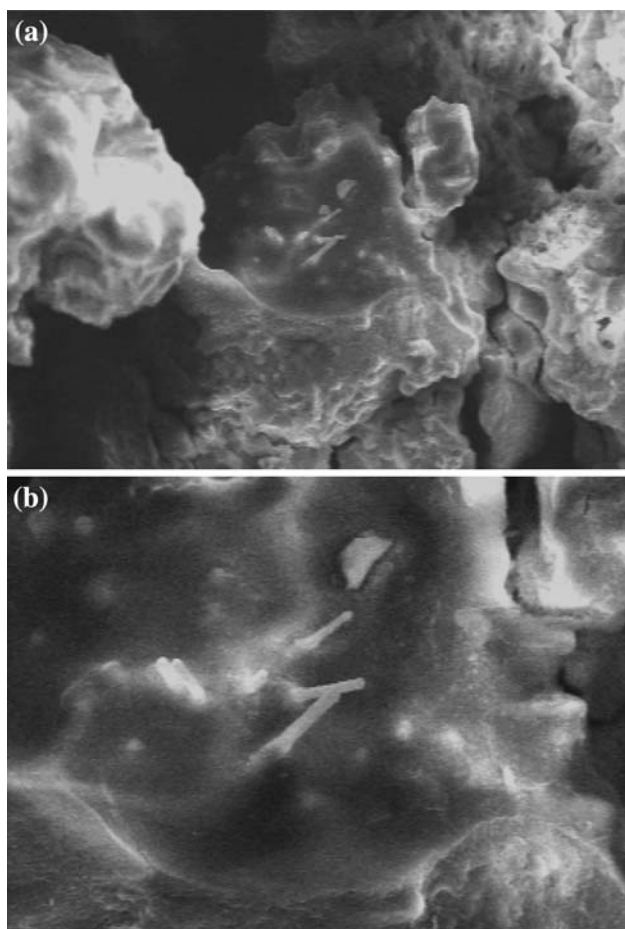


Fig. 11 SEM Pozzolanelle: **a** MF 177X; **b** 456X

thawing and then by hand. In both cases, the material was oven-dried at 105°C before the grain size distribution was determined by dry sieve analysis.

The first technique was only effective for the Pozzolanelle, while the second technique was adopted for both Pozzolanelle and Conglomerato Giallo. While the grain size distribution of Pozzolana Nera and Conglomerato Giallo is not affected by the sieving time or number of sieving cycles, the grain size distribution obtained for the Pozzolanelle depended on the number of sieving cycles, with a tendency for the fine fraction to increase with increasing number of cycles, indicating imperfect separation of small aggregates. The grain size distribution curve obtained with this procedure stabilizes after about 5 sieving cycles. A much more pronounced shift of the grain size distribution is observed for cycles of freezing and thawing, showing how the second procedure is much more effective in breaking the original structure of the material. Again, after three cycles of freezing and thawing the grain size distribution of Pozzolanelle tends to stabilise.

Figure 13 shows the grain size distribution obtained for the three materials. The Pozzolana Nera is a well graded

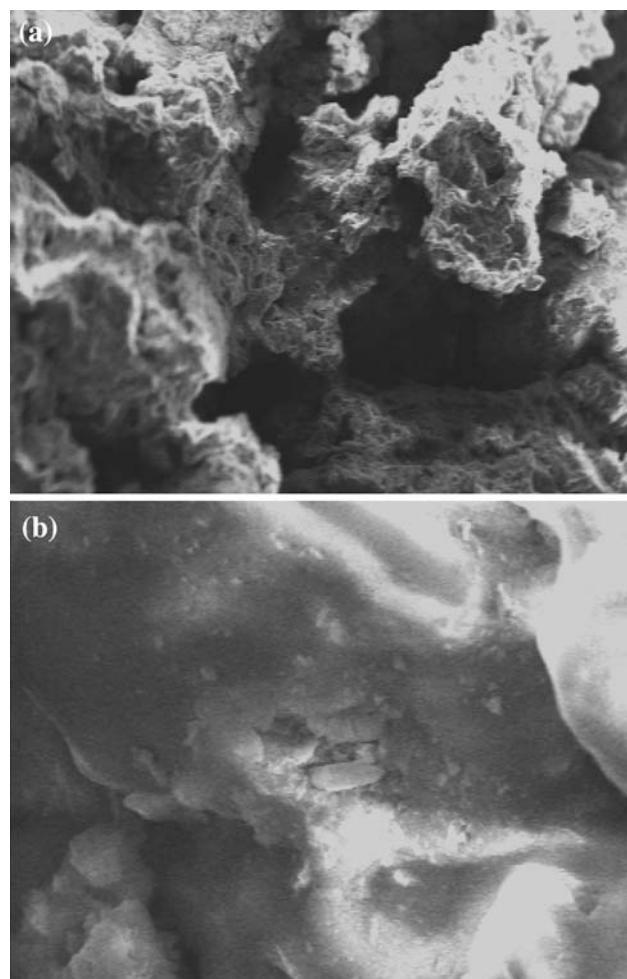


Fig. 12 SEM Conglomerato Giallo: **a** MF M40X; **b** MF 1530X

gravel with sand, with a coefficient of uniformity $U = 34$, $D_{10} = 0.12$ mm, and $D_{60} = 4.08$ mm. The Pozzolanelle are gravels with sand, with a coefficient of uniformity $U = 15$, $D_{10} = 0.54$ mm, and $D_{60} = 7.94$ mm; the Conglomerato Giallo is a gravel with sand, with a coefficient of uniformity $U = 5$, $D_{10} = 0.71$ mm, and $D_{60} = 3.69$ mm.

Specific gravity was measured on the whole material and on increasingly finer powdered material using a helium picnometer. The results obtained for all three materials are summarised in Fig. 14 together with similar results obtained on expanded clay pellets, commercially known as Leca, characterised by very high values of closed porosity (Gagliardi 2002). The data for the Pozzolanelle do not show a clear trend of specific gravity with grain size, with a scatter $<2\%$; the calculated vesiculation index is nil. For both the Conglomerato Giallo and the Pozzolana Nera, a small increase in specific gravity with decreasing particle diameter is observed over the investigated range of diameters (about 4.08% for Conglomerato Giallo and about 2.38% for the Pozzolana Nera. The computed values of

Table 2 Main physical properties of the materials under investigation

Material	w/c (%)	G_s (-)	γ (kN/m ³)	γ_d (kN/m ³)	n (-)	S_r (%)
Pozzolana Nera	13.0 ± 1.7	2.69	16.46 ± 0.06	14.64 ± 0.03	0.45 ± 0.01	43.5 ± 3.5
Pozzolanelle	16.3 ± 1.9	2.74	11.92 ± 0.06	9.93 ± 0.03	0.64 ± 0.01	25.0 ± 5.2
Conglomerato Giallo	26.8 ± 0.6	2.45	17.40 ± 0.06	17.40 ± 0.03	0.29 ± 0.01	88.0 ± 1.5

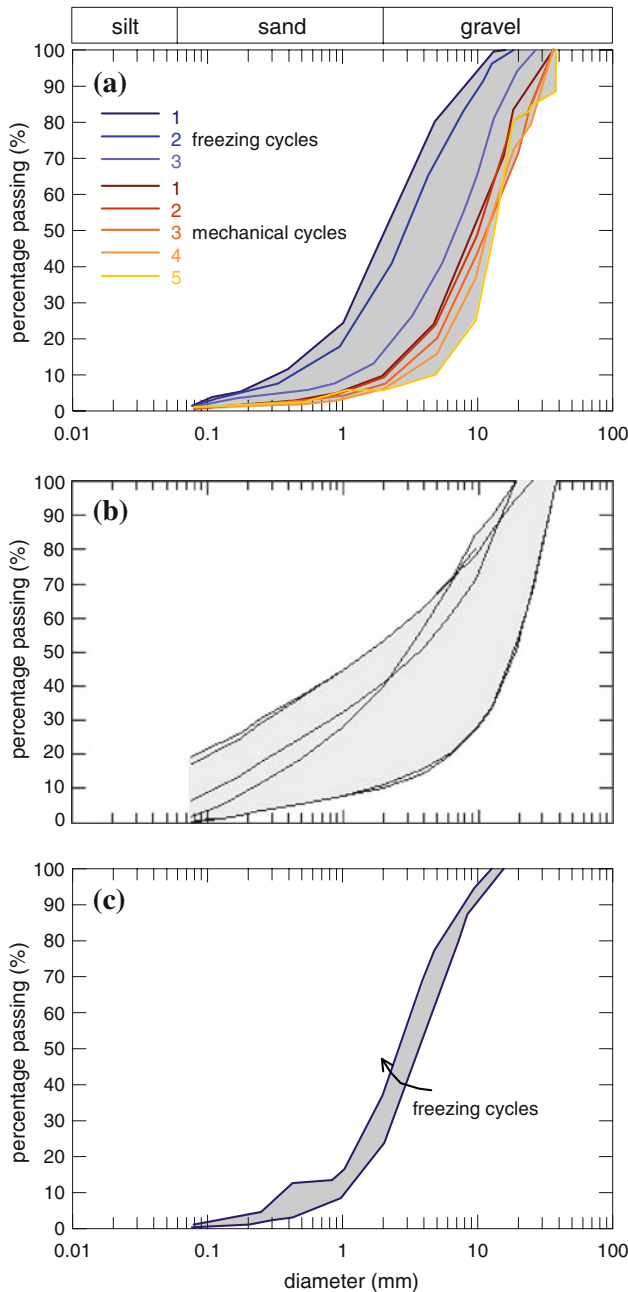


Fig. 13 Grain size distribution: **a** Pozzolanelle; **b** Pozzolana Nera (adapted from Cecconi 1999); **c** Conglomerato Giallo

vesiculation index are $V = 3.31\%$ and 2.26% , respectively. For all three materials the vesiculation index is less than 5% (not vesiculated), demonstrating the marginal role

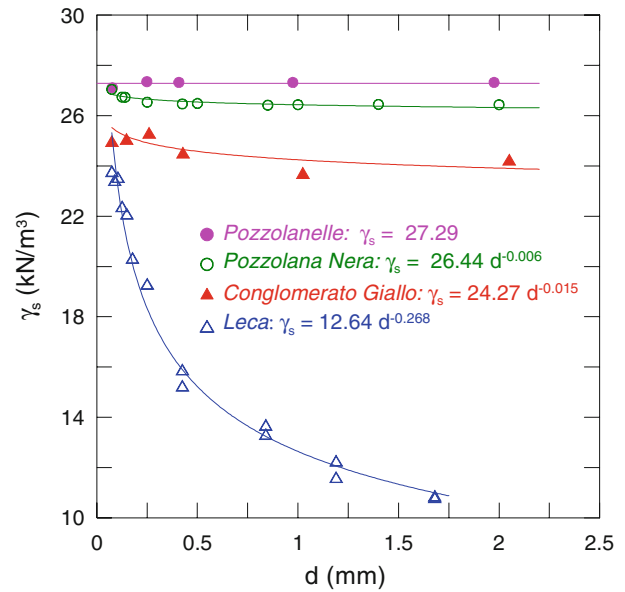


Fig. 14 Dependence of γ_s on grain size for the three materials under investigation

played by closed porosity. In contrast, the expanded clay pellets have a vesiculation index $V = 54.52\%$ (medium vesiculation).

Experimental programme

The core of the experimental work consisted of direct shear tests on intact samples of Pozzolanelle. A smaller number of one-dimensional compression, uniaxial compression and indirect tension tests on intact and reconstituted samples of Pozzolanelle and Conglomerato Giallo were also carried out, to determine the compressibility of the two materials and the strength of the intact Conglomerato Giallo.

The direct shear tests were carried out in standard 60×60 mm shear boxes. However, samples of 40 mm were used to avoid the rupture surface crossing the boundaries of the shear box. The shear force was developed by an electric motor, providing a variable speed ranging from 5×10^{-4} to 2 mm/min. All tests were performed at a displacement rate of 0.1 mm/min. Micrometer dial gauges with a resolution of 0.001 and 0.01 mm were used to measure vertical and horizontal displacements respectively. One dimensional compression tests were carried out in

standard oedometer cells with a diameter of 71.4 mm, to a maximum vertical stress of about 4,000 kPa, or in reduced diameter (35.1 mm) cells to a maximum vertical stress of 12,800 kPa.

For the direct shear and oedometer tests, intact samples of Pozzolanelle were obtained manually from partially saturated natural blocks by pushing a square or circular thin-walled soil sampler into the block and trimming the material around it with a knife. To ensure good contact between the sample and the loading system any voids or irregularities were filled with a mix of 85% crushed Pozzolanelle passing sieve N40 and 15% alabastrine gypsum. Direct shear tests were carried out on both vacuum dried and saturated natural samples; the latter were placed into the shear box, submerged in water and saturated under vacuum. Reconstituted samples of Pozzolanelle and Conglomerato Giallo for oedometer testing were formed using material passing ASTM sieve 10 (2 mm) which was oven-dried, mixed with de-aired distilled water at a water content $\cong 20\%$ and compacted in the oedometer in thin layers.

Intact samples of Conglomerato Giallo for uniaxial compression and indirect tension tests were obtained by rotary coring partially saturated natural blocks. Before coring, the blocks were immersed in water, which increased the saturation degree up to $S_r \cong 0.7$, and then frozen at -20°C ; the ends were then squared on a band saw up to a tolerance of 0.2 mm which, for the grain size distribution of the material, is the smallest achievable.

The effects of freezing on the microstructure of the material were partially investigated by means of compression wave velocity measurements as the velocity with which stress waves are transmitted through a soil depends on the elastic properties and density of the material. The velocity of propagation of P-waves has been traditionally related to the degree of fissuring and micro-cracking of rock masses (Goodman 1989). In this case a significant reduction of the velocity of propagation of P-waves would indicate a reduction of the initial stiffness of the material, probably due to the de-structuring induced by freezing. Measurements of P-wave velocity were first made on vacuum dried natural samples of approximate dimensions of $0.15 \times 0.15 \times 0.15$ m. P- and S-waves were transmitted and received across unconfined samples using electro-mechanical 15 mm diameter transducers with a characteristic frequency of vibration of 1 MHz under an axial load of 1.0 kN for the Conglomerato Giallo and of 0.8 kN for the Pozzolanelle.

For the Conglomerato Giallo the measurements were repeated on the same samples after they had been immersed in water, frozen at -20°C , thawed and vacuum dried; the procedures and the times for saturation and freezing were the same as those employed for the preparation of laboratory samples. The results showed the effects

of freezing on the stiffness properties of the Conglomerato Giallo to be very minor, with a reduction of the P-wave velocity of about 3%. For Pozzolanelle one cycle of freezing and thawing causes the complete loss of cohesion of the material so it was not possible to prepare undisturbed samples by this technique nor to repeat the measurements after freezing and thawing.

Main results

Strength

The strength of intact Pozzolanelle was investigated by direct shear tests carried out at increasing vertical effective stress from $\sigma'_v = 10$ to 400 kPa. The shear stress–horizontal displacement curves ($\tau - \delta x$) are shown in Figs. 15, 16, 17, 18. It can be seen that the shear strength of the dry material is larger than that of the saturated material. At all levels of vertical effective stress, the dry material has a brittle and pronounced dilatant behaviour. The saturated material shows a more ductile behaviour and a reduced tendency to dilate, even if truly compressional behaviour is only observed at vertical effective stresses larger than 200 kPa.

The maximum values of shear stress (τ_{\max}) are plotted in Fig. 19 in a conventional Mohr–Coulomb plot, as a function of vertical stress, σ'_v . Two linear failure envelopes were used to define the peak shear strength parameters of the material in dry and saturated conditions. The cohesion intercept is about 270 kPa in the dry condition, and reduces to 80 kPa when the degree of saturation approaches unity. The peak friction angle is about 36° for both states.

Figure 20 shows the end-of-test failure envelopes. No information about critical states can be inferred from the data as all curves in Figs. 15, 16, 17, 18 are plotted for horizontal displacements lower than about 3–4 mm. Data obtained at larger displacements have been intentionally omitted due to their unreliability. The experimental data in both the dry and saturated conditions indicate that the value of the peak friction angle is the same as that at the end-of-test condition.

At the end of each direct shear test, the two halves of the shear box were separated carefully in order to be able to observe the shape of the shear failure surface. This may be more or less even (see Fig. 21a and b), depending on the presence of stronger lithic elements or scorias, but not on the value of the vertical effective stress. The shape of the failure surface of all samples was systematically recorded along three sections using a profilometer (Barton comb), as in the examples in Fig. 22. Sample 2, tested at $\sigma'_v = 10$ kPa, is representative of the average roughness exhibited by the majority of samples, while sample 6,

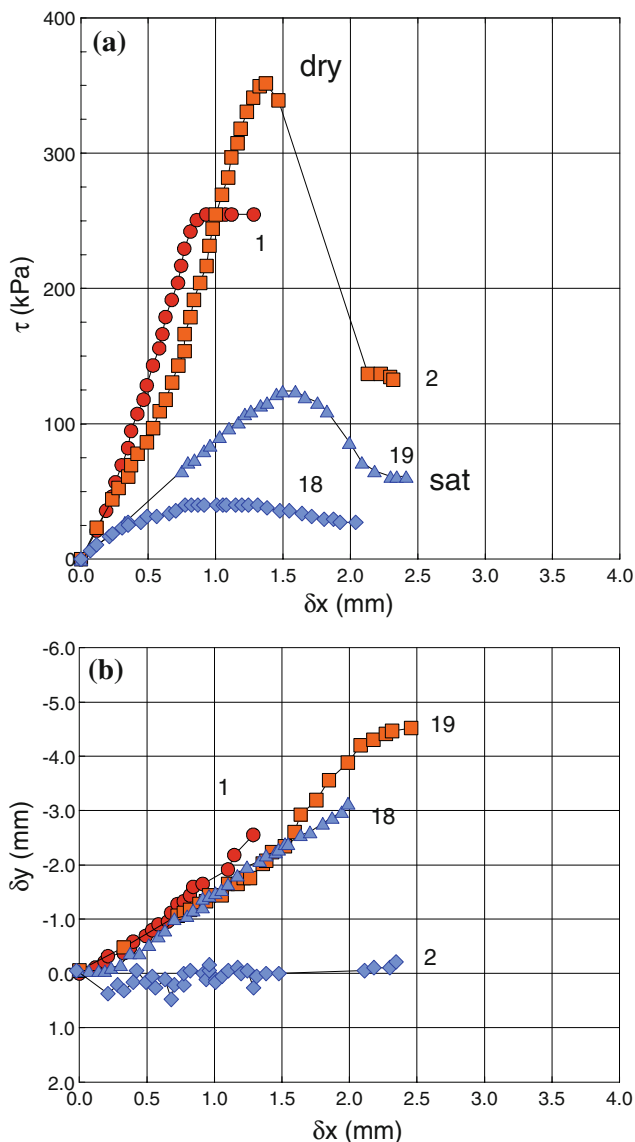


Fig. 15 Direct shear test results, $\sigma'_n = 10$ kPa: **a** shear stress τ —horizontal displacement δx ; **b** vertical displacement δy —horizontal displacement δx

tested at $\sigma'_v = 100$ kPa, is an extreme, although not unique case, in which the shape of the sliding surface is very uneven. Comparison with standard roughness profiles from Barton and Choubey (1977), each corresponding to a narrow range of values of the joint roughness coefficient (JRC), revealed that for dry samples JRC values are in the range 18–20, larger than that observed for saturated samples, explaining the higher values of dilatancy of dry samples. Also, the shape of the failure surface of sample 6 demonstrates clearly the need to use increased height samples to avoid interference between the same failure surface and the sides of the shear box.

Particle size analysis was carried out on the material taken from the plane of failure of direct shear tests

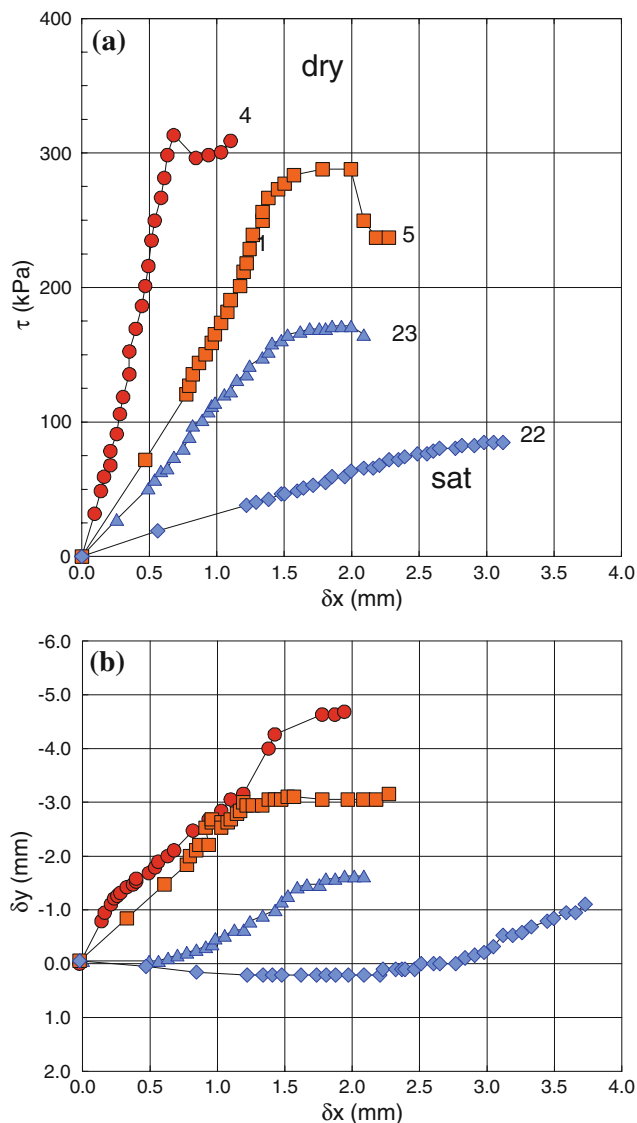


Fig. 16 Direct shear test results, $\sigma'_n = 50$ kPa: **a** shear stress τ —horizontal displacement δx ; **b** vertical displacement δy —horizontal displacement δx

performed on intact samples of Pozzolanelle. The resulting grading curve (Fig. 23) is more uniform than that of the original material, with a $D_{60} = 2.696$ mm, $D_{10} = 0.1193$ mm and $U = 23$. The coarser fraction—from 5 to 20 mm—is completely absent. This implies that the formation of the shear plane during the test is connected to the breakage of both the inter-granular bonding inside the matrix and the larger and weaker clasts, such as scoria and pumices.

No direct shear tests on intact samples of Conglomerato Giallo were carried out as part of this investigation. The strength of the natural material was obtained by unconfined compression tests and indirect (Brazilian) tension tests on rotary cored cylindrical samples. Figure 24 shows the

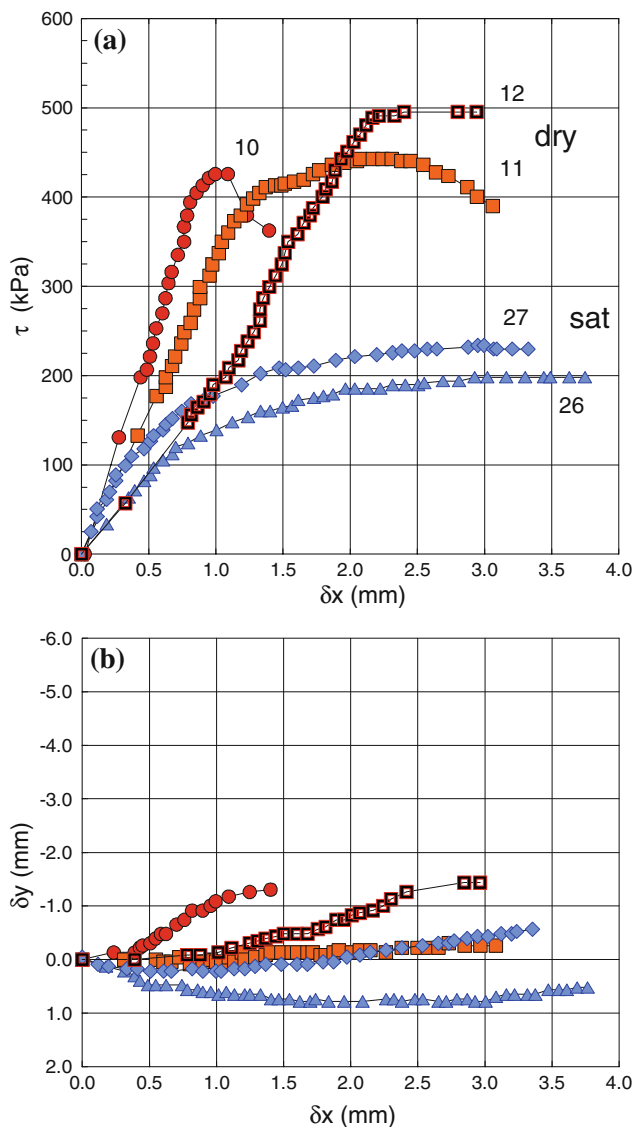


Fig. 17 Direct shear test results, $\sigma'_n = 200$ kPa: **a** shear stress τ —horizontal displacement δx ; **b** vertical displacement δy —horizontal displacement δx

results of unconfined compression tests for three natural samples of Conglomerato Giallo. All samples showed brittle failure by axial splitting; the small differences between the maximum values of axial stress at failure can be attributed to natural variability of the material. The average value of compression strength is $\sigma_c = 4.3$ MPa, ie the material can be classified as a weak rock (Anon 1970). Figure 25 shows the tangent stiffness, E , of the material in uniaxial compression as a function of the logarithm of axial strain. The initial average value of the stiffness of the material is about 300 MPa, followed by gradual stiffening up to 700 MPa and then by a reduction of E as strain increases, as commonly observed in soft rocks. As seen in Fig. 26 the average tensile strength value is 580 kPa, or

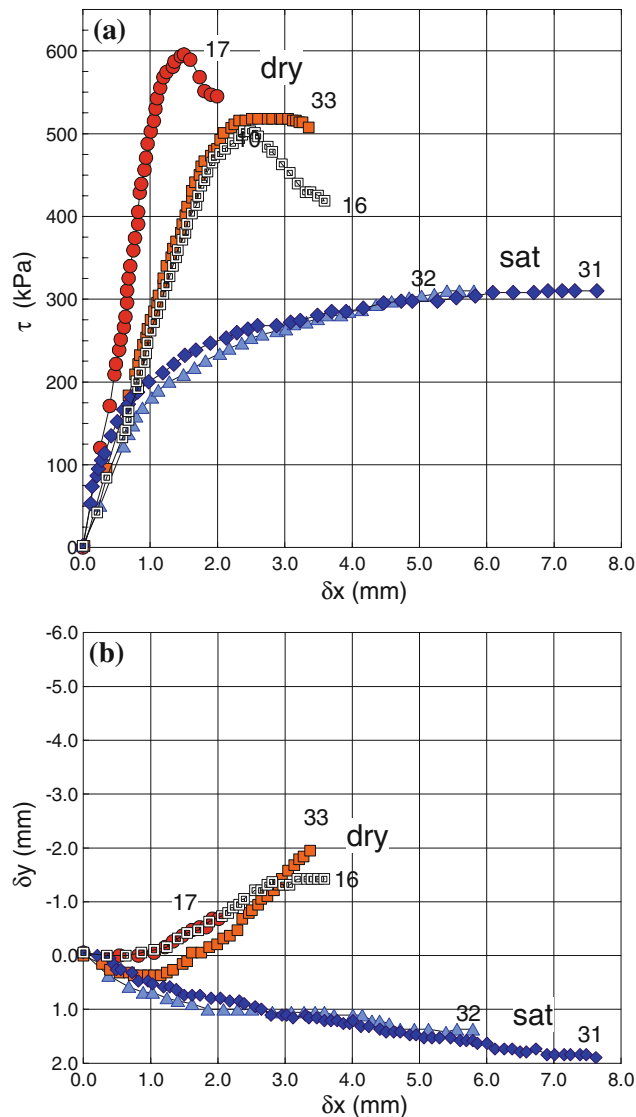


Fig. 18 Direct shear test results, $\sigma'_n = 400$ kPa: **a** shear stress τ —horizontal displacement δx ; **b** vertical displacement δy —horizontal displacement δx

about one tenth of the compressive strength. The tensile stiffness is plotted versus logarithm of axial strain in Fig. 27, which shows a very similar trend to the compressive stiffness. However, absolute values increase from an initial value of about 30 MPa to a maximum of about 70 MPa followed by a gradual reduction of stiffness as strain increases. The strength of Conglomerato Giallo is described using Hoek and Brown (1980) failure criterion:

$$\sigma_1 = \sigma_3 + \sigma_{ci} \left(m \frac{\sigma_3}{\sigma_{ci}} + s \right)^{0.5}$$

where σ_1 and σ_3 are the major and minor effective principal stresses at failure, σ_{ci} is the uniaxial compressive strength of the intact rock material, and m and s are material

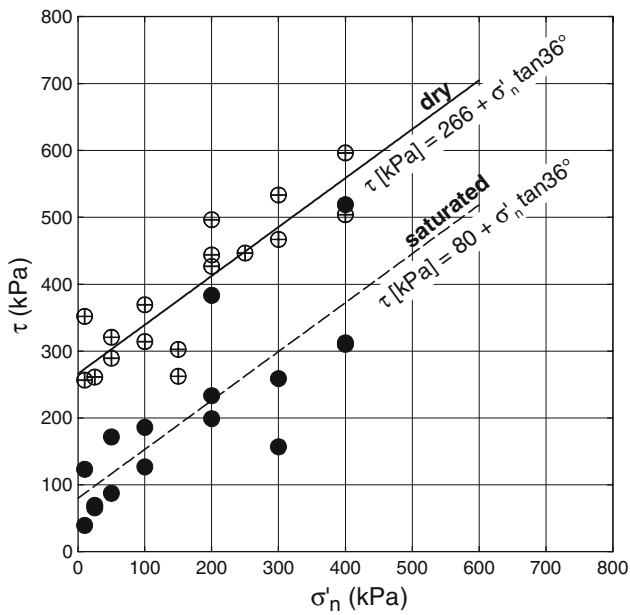


Fig. 19 Peak failure envelopes for dry and saturated Pozzolanelle

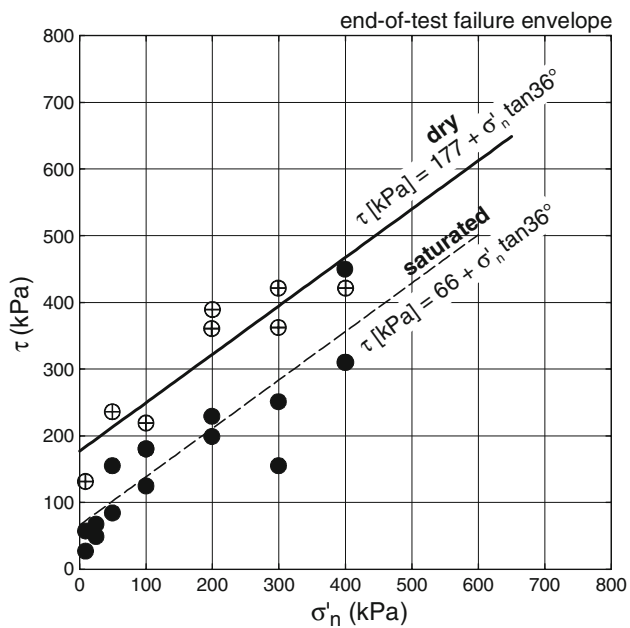


Fig. 20 End-of-test failure envelopes for dry and saturated Pozzolanelle

constants. The uniaxial compressive strength is obtained by setting $\sigma_3 = 0$, giving:

$$\sigma_c = \sigma_{ci} s^{0.5}$$

In this case $\sigma_{ci} = \sigma_c$, and, therefore, $s = 1$ (intact rock). Hoek (1968) showed that, for brittle materials, the uniaxial tensile strength is equal to the biaxial tensile strength, obtained by setting $\sigma_1 = \sigma_3 = 0$, yielding:

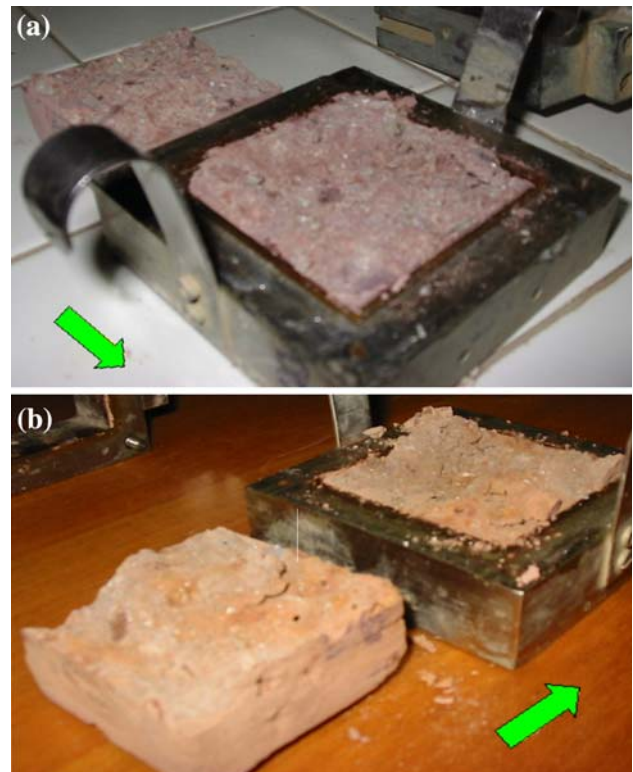


Fig. 21 Example of (a) “even” (b) “uneven” shear failure surface

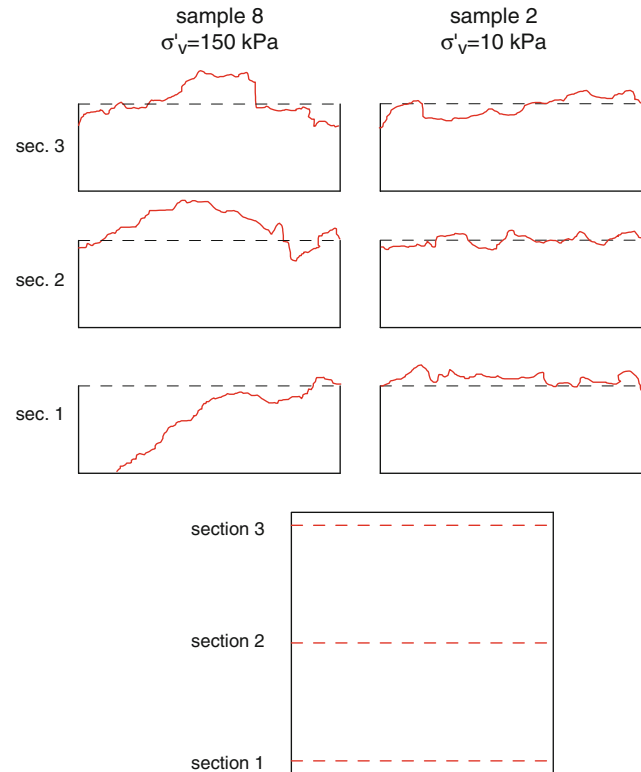


Fig. 22 Example of shear failure surface. At the bottom, a plan view of the sample (60 × 60 mm)

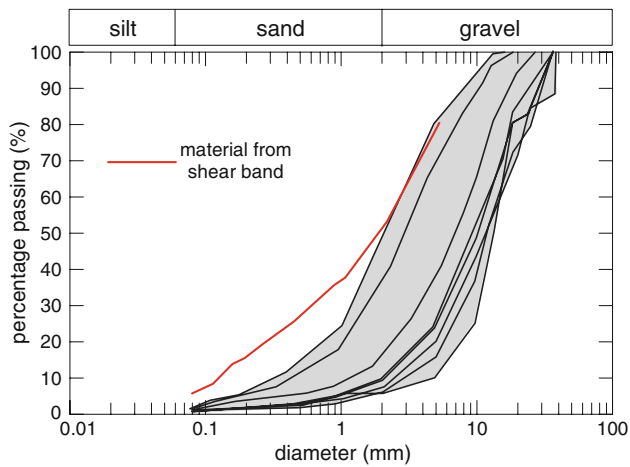


Fig. 23 Pozzolanelle: grain size distribution of material from shear band

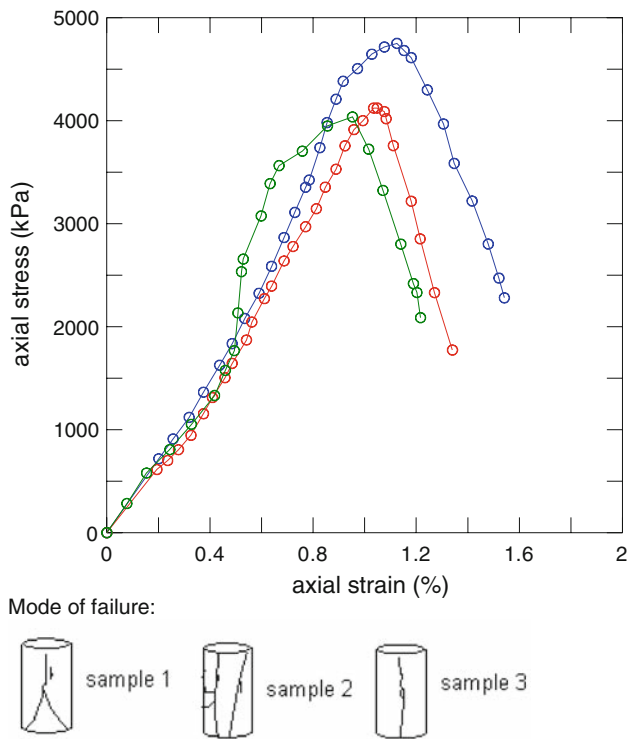


Fig. 24 Stress strain behaviour of Conglomerato Giallo from uniaxial compression tests

$$\sigma_t = -s \frac{\sigma_c}{m} \quad \text{or} \quad m = -\frac{\sigma_c}{\sigma_t} = 7.41$$

The strength envelope is shown in the Mohr plane in Fig. 28, together with the equivalent Mohr-Coulomb failure criterion obtained by fitting an average linear relationship to the Hoek and Brown strength envelope (Hoek et al. 2002). The equivalent Mohr Coulomb cohesion intercept is about 936 MPa and the equivalent friction angle is about 39.57°.

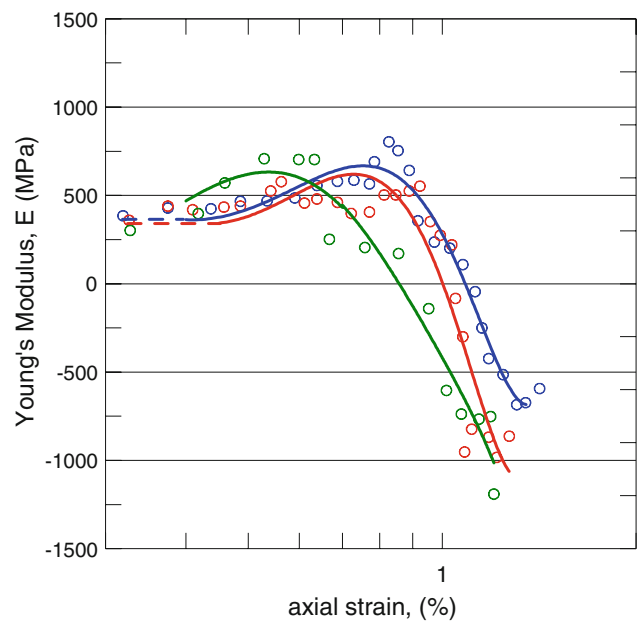


Fig. 25 Stiffness of Conglomerato Giallo from uniaxial compression tests

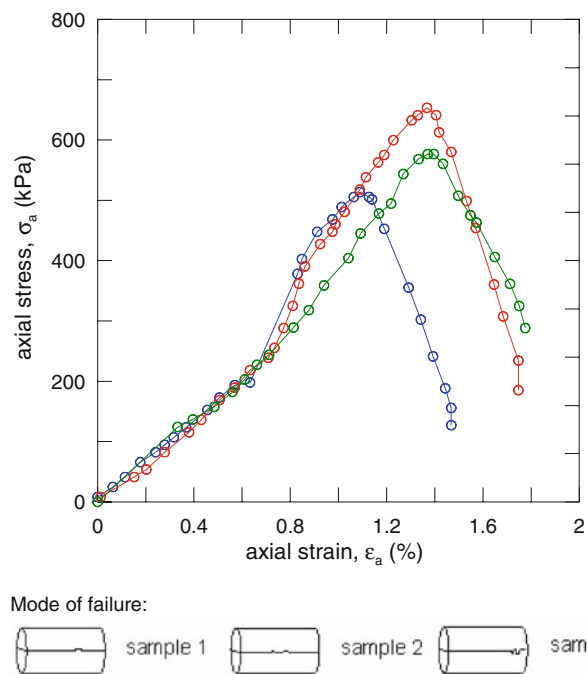


Fig. 26 Stress strain behaviour of Conglomerato Giallo from indirect tension tests

Compressibility

Figure 29 shows the results of three one-dimensional compression tests on intact samples of Pozzolanelle, as voids ratio (e) versus logarithm of vertical effective stress (σ'_v). The initial voids ratio of intact samples is in the range $e = 1.7 \pm 0.1$. The initial response on first loading is

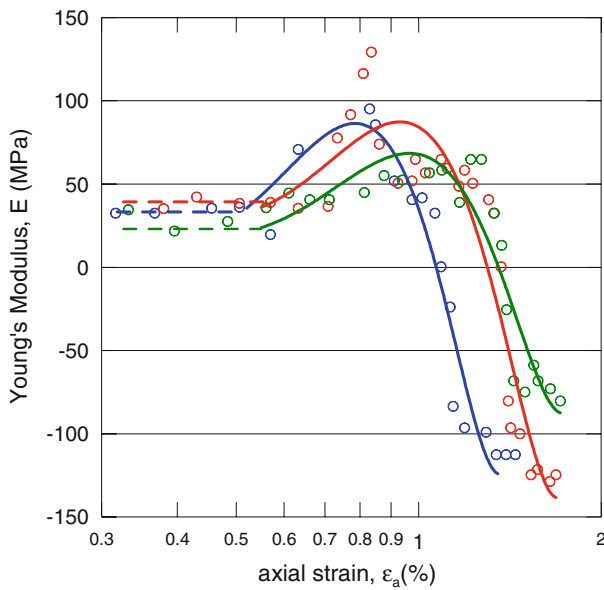


Fig. 27 Stiffness of Conglomerato Giallo from indirect tension tests

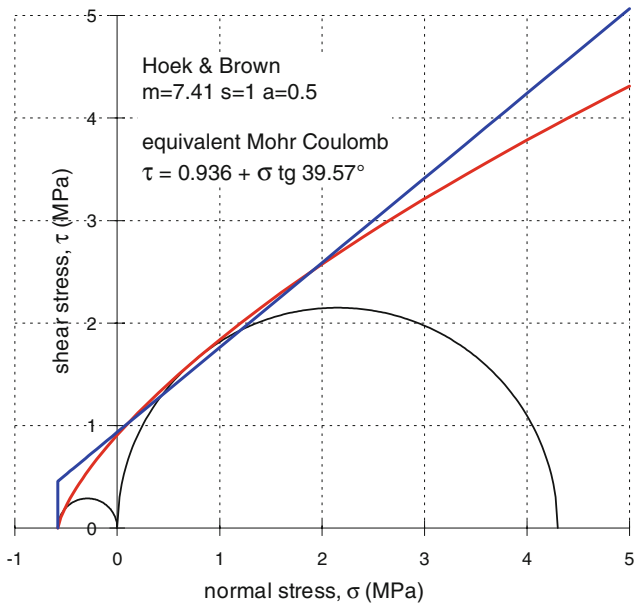


Fig. 28 Strength envelope for Conglomerato Giallo

characterized by gradual yield as the vertical effective stress increases. The values of the yield stress (σ'_y), determined using Casagrande's procedure, are shown as arrows in Fig. 29. It can be seen that for the three tested samples σ'_y varied from 2,290 to 3,160 kPa. For vertical effective stresses in excess of about 3 MPa, large volume strains occur along a single normal compression line (solid line in Fig. 29), characterised by a compression index $C_c = 0.86$. The response on unloading is always very stiff, with an average swelling index (C_s) of 0.039.

Figure 30 shows the results of two tests on reconstituted samples of Pozzolanelle, together with the same data as

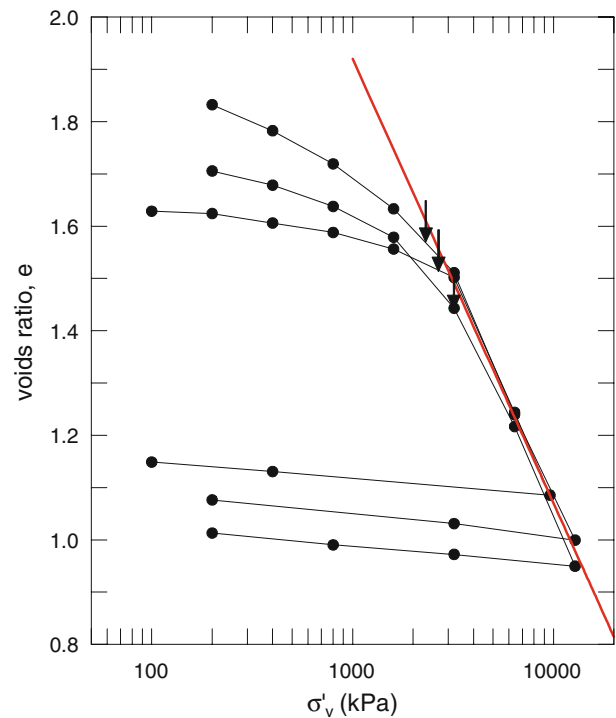


Fig. 29 Results of one-dimensional compression tests for natural samples of Pozzolanelle

Fig. 29. The largest initial voids ratio that it was possible to achieve for the reconstituted samples by compaction in the mould ($e = 1.453$) is below the range of values measured for intact samples; the compression curve of the reconstituted samples is also below that obtained for the natural samples. The values of the compression index obtained from the last two points of the compression curve decrease with decreasing initial voids ratio, although it is likely that for the densest sample this is an underestimate of the true value of C_c , as the state of the sample has not yet entered virgin compression. On unloading, the behaviour of the reconstituted samples is stiffer than that of the natural samples with an average value of $C_s = 0.022$. Figure 30 also shows the results from one natural sample of Pozzolanelle that has undergone one cycle of freezing and thawing. The initial voids ratio of the sample is at the lower bound of the range for most natural samples. However the response of the sample on first loading is less stiff than that of other intact natural samples, probably due to partial destructuring induced by freezing and thawing.

No oedometer tests were carried out on intact samples of Conglomerato Giallo. Figure 31 shows the results of three one-dimensional compression tests on reconstituted samples of Conglomerato Giallo, as voids ratio versus logarithm of vertical effective stress. The three samples were reconstituted at three values of initial voids ratio in the range $e = 1.236$ to 1.864. The response on first loading is characterised by gradual yield as the vertical effective

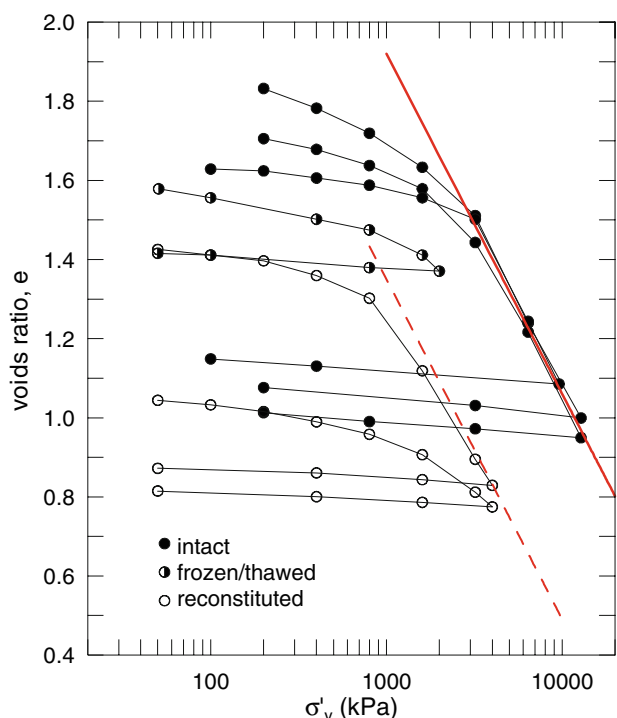


Fig. 30 Results of oedometer compression tests for natural and reconstituted samples of Pozzolanelle

stress increases. The values of the compression index obtained from the last two points of the compression curves decrease with decreasing initial voids ratio, although it is likely that for the densest sample this is an underestimate of the true value of C_c , as the state of the sample has not fully entered virgin compression. On unloading, the behaviour of the reconstituted samples is stiffer than on first loading with an average value of $C_s = 0.022$.

Figure 32 shows the C_c values obtained from tests on intact and reconstituted samples of the three materials versus their initial voids ratio together with experimental data obtained for other natural soils and weak rocks (Croce et al. 1961; Vaughan 1988). A linear increase in compressibility with initial voids ratio is observed for both intact and reconstituted samples.

Creep

Like other Italian pyroclastic soils and weak rocks (Croce 1954; Evangelista and Aversa 1994) the materials under investigation may exhibit significant long term deformation due to creep. This was investigated by performing conventional oedometer tests on both natural and reconstituted samples. Some results for the secondary one-dimensional compression of Pozzolana Nera (Cecconi et al. 2005) are compared with the results from the other two deposits investigated.

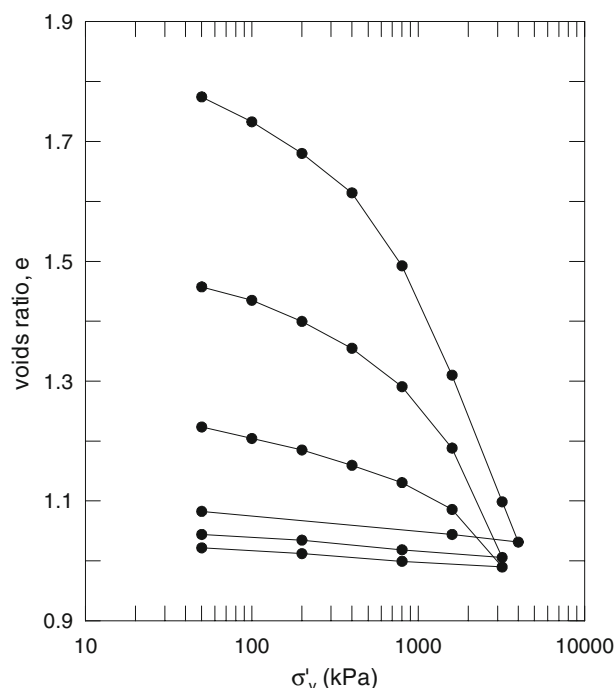


Fig. 31 Results of oedometer compression tests for reconstituted samples of Conglomerato Giallo

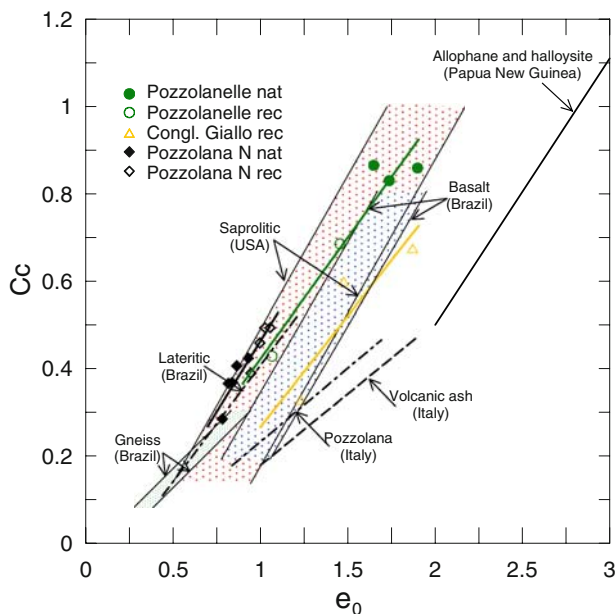


Fig. 32 Dependence of compression index on initial voids ratio for several hard soils soft rocks (literature data from Vaughan 1988 and Croce et al. 1961)

The rate of strain during primary creep was described using the secondary compression index on first loading, C_{z_2} , conventionally estimated as the slope of the e - $\log t$ curve in the logarithmic cycle following the end of primary consolidation (t_{90}) (Mesri et al. 1978; Mesri and Godlewski 1977):

$$C_\alpha = -\frac{\Delta e}{\Delta \log t}, \text{ on loading } \Delta e < 0 \Rightarrow C_\alpha > 0$$

Time t_{90} was computed using the method suggested by Taylor (1948) and varied between 10 and 30 s. After primary consolidation during the log-cycles following t_{90} , the secondary compression and swelling indexes remained approximately constant with time. Figure 33 shows the variation of C_α with vertical effective stress on first loading for the three materials under investigation. The experimental data are fitted by power functions (see Table 3):

$$C_\alpha = \beta \sigma'_v{}^\alpha$$

in which β and α are fitting parameters, whose numerical values depend on the units adopted to express σ'_v .

Concluding remarks

This paper describes the results of an experimental investigation of the engineering geological properties of three pyroclastic deposits from the Colli Albani volcanic complex, typical of the subsoil of Rome (Italy). In their natural state, these materials are coarse-grained weak rocks, generally unsaturated in situ.

A technical sheet for the description and classification of these deposits was developed during the experimental work and is presented in the paper. The sheet provides a useful index to follow for the standard description of pyroclastic soils and a support for the engineering geologist to define qualitatively and semi-quantitatively some preliminary properties of the material.

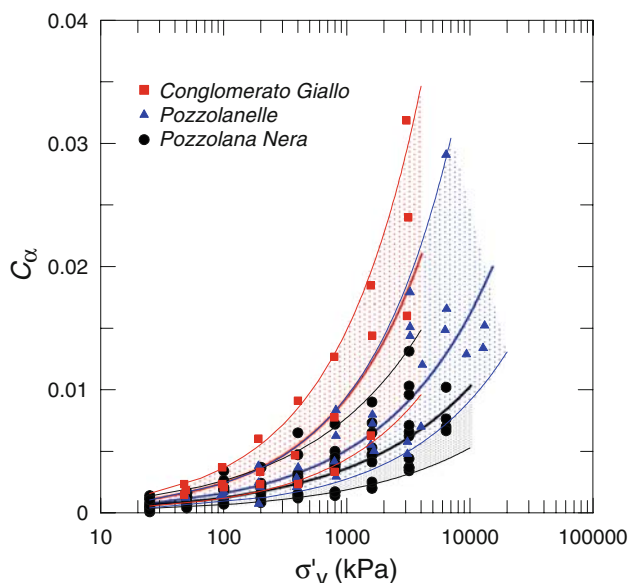


Fig. 33 Dependence of C_α on σ'_v for the three materials under investigation

Table 3 Creep parameters α and β for the three materials under investigation

Material	α (-)	β (1/kPa $^\alpha$)
Pozzolana Nera	0.448	1.67×10^{-4}
Pozzolanelle	0.498	1.67×10^{-4}
Conglomerato Giallo	0.575	1.77×10^{-4}

The experimental investigation consisted mainly of identification and classification tests, one-dimensional compression and direct shear tests on saturated and dry samples of Pozzolanelle and Conglomerato Giallo. An investigation of the micro-structural features of the materials was also undertaken by means of optical and electron scanning microscopy. Unlike other pyroclastic materials, pyroclastic flow deposits from the Colli Albani exhibit a very small closed porosity within the clasts.

The measurement of the physical properties and mechanical characteristics of the materials was carried out using conventional laboratory techniques with the goal of identifying some of the problems that may be encountered in the laboratory characterisation and to assist in the choice of suitable testing programmes. Due to the nature of the soils, however, non-standard techniques were developed for sample preparation and testing.

The procedures adopted to prepare the material for sieving significantly affect the experimental grain size distribution curve. For welded pyroclastic rocks, such as Pozzolanelle and Pozzolana Nera, the material can be broken by a weak mechanical action such as that applied by human hands, which is sufficient to separate aggregates but not strong enough to break individual particles. However, at the lower bound of welded pyroclastic rocks (Pozzolanelle), the grain size distribution of the material obtained by hand separation is often still significantly affected by the number of sieving cycles, testifying imperfect separation of aggregates. Subjecting the material to cycles of freezing and thawing before hand separation was found to be very effective in separating larger aggregates; only a small number of thermal cycles (three in the case of Pozzolanelle) being sufficient for the grading curve to stabilise. Moreover, for lithoid or semi-lithoid pyroclastic rocks, such as the Conglomerato Giallo, the material can only be broken by hand after the original structure of the rock has been weakened by cycles of freezing and thawing.

Sample preparation for mechanical testing is a very delicate issue. Cylindrical samples of lithoid and semi-lithoid pyroclastic rocks, such as the Conglomerato Giallo, may be obtained by rotary coring partially saturated frozen natural blocks. The technique was originally developed and successfully used for the Pozzolana Nera, at the upper

bound of welded pyroclastic rocks. In both cases, the effects of freezing on the microstructure, as revealed by measured values of compression wave velocity through the samples, are negligible. The technique, however, proved completely ineffective for other welded pyroclastic rocks, such as the Pozzolanelle, whose structure is completely destroyed by even one cycle of freezing and thawing. In this case, intact samples can only be prepared by pushing circular or square (for direct shear) thin-walled samplers into the natural blocks and trimming the material around it with a knife. This is a very wearisome and time consuming procedure; an alternative reported in the literature is that of double-barrel coring of natural samples without freezing (Diano 2005) although this was not undertaken in the present study.

From the point of view of grading, all the tested materials were gravel with sand. However, quite often larger lithic fragments were present in the matrix, causing small jerks and jolts in the observed response; note for example the sharp increase of stiffness during unconfined compression of sample 2 at about 0.5% axial strain. The shape of the shear surfaces of direct shear tests is also strongly affected by the occurrence of larger fragments. In some cases it can be so uneven as to intersect the sides of the box, e.g. sample 8, tested at 150 kPa vertical stress. For all these reasons it is recommended that larger samples are used.

Direct shear tests on natural samples of Pozzolanelle indicate that the strength of the saturated material is affected very significantly by dilation, both at peak stress and at the end of test as the horizontal displacements imposed in the shear box are far too small to reach constant volume shearing. On the other hand, for the material at the natural water content, the large values of measured cohesion may be attributed to a combination of increased dilation (due to the roughness of the shear surface) and suction.

The results of the oedometer tests confirm that the initial voids ratio is the main factor affecting the compressibility of these materials, with an almost linear increase of C_c with e_0 . The trends obtained for the three materials under investigation are consistent with literature data for other natural soils and weak rocks. Like many pyroclastic soils and weak rocks all three materials exhibit significant long term deformations due to creep.

Acknowledgments The authors are grateful to Tatiana Rotonda of Roma La Sapienza and Marco Marinelli of Roma Tor Vergata, who made available the experimental set-up and their expertise on how to carry out elastic wave measurements and SEM analyses respectively. Francesca Bozzano and her group were the source of much valuable information on the geology of the Colli Albani. The authors also wish to thank the technical staff at Geoplanning S.r.l. for their help with the experimental work and Mr Tozzi, owner of I.MA.TER. quarry.

SITE: CAVA IMETER- ROMA OPERATOR: GEOL. M. SCARAPAZZI DATE: 22/02/08	
1. STATION: Nord side, 2. LAYER: D1 (Pozzolanelle), 3. THICKNESS: 5.7 m, 4. ORIENTATION: N 30° E 10 SE	
5. PYROCLASTIC TYPE <input type="checkbox"/> Lithoid <input checked="" type="checkbox"/> Welded <input type="checkbox"/> Granular <input type="checkbox"/> Altered <input type="checkbox"/> Deeply altered	
6. COLOUR Matrix: dry pinkish-white (Munsell cod 7.5 YR 8/2) wet pinkish-grey (Munsell cod 7.5 YR 6/2) Clasts: dry light reddish-brown (Munsell cod 2.5 YR 6/3 e 6/4) wet reddishbrown (Munsell cod 2.5 YR 4/3 e 4/4)	
7. SEDIMENTARY STRUCTURE <input type="checkbox"/> Stratified <input type="checkbox"/> Graded <input type="checkbox"/> Laminated <input checked="" type="checkbox"/> Massive <input checked="" type="checkbox"/> Homogeneous <input type="checkbox"/> Not homogeneous	
8. CLAST NATURE <input checked="" type="checkbox"/> >90% Juvenile <input type="checkbox"/> 60% Matrix <input type="checkbox"/> <10% Secondary <input type="checkbox"/> 30% Clasts <input type="checkbox"/> 20% Scoria <input type="checkbox"/> 5% Pumices <input type="checkbox"/> 5% Crystals <input type="checkbox"/> rare% Other (accidental sedimentary/ xenoliths / sedimentary)	
9. TEXTURE <input type="checkbox"/> Granular sustained <input checked="" type="checkbox"/> Intermediate <input type="checkbox"/> Matrix sustained	
10. CLAST ORIENTATION <input checked="" type="checkbox"/> Isotropic <input type="checkbox"/> Anisotropic <input type="checkbox"/> Imbricated (Attitude)	
11. GRADING Blocks / Bombs (d > 2mm) 0% Lapillus (2 - 4mm) 50% Coarse ash (0.063 - 2 mm) 40% Medium to Fine ash (< 0.063 mm) 10%	
12. ANGULARITY <input type="checkbox"/> Very angular <input type="checkbox"/> Angular <input checked="" type="checkbox"/> Subangular <input type="checkbox"/> Subrounded <input type="checkbox"/> Rounded <input type="checkbox"/> Very rounded	
13. VESICULATION <input type="checkbox"/> High <input type="checkbox"/> Medium <input checked="" type="checkbox"/> Low <input type="checkbox"/> Absent	
14. POROSITY <input checked="" type="checkbox"/> High <input checked="" type="checkbox"/> Medium <input type="checkbox"/> Low	
15. BONDING <input checked="" type="checkbox"/> True <input type="checkbox"/> Electrostatic <input checked="" type="checkbox"/> Apparent <input checked="" type="checkbox"/> Welding <input type="checkbox"/> Low <input type="checkbox"/> Absent <input type="checkbox"/> Medium <input checked="" type="checkbox"/> High	
NOTES: 8 = Determination made by visual analysis, are recognizable minerals of leucite. 11 = Granulometry determined by sieving and sedimentation analysis. 14 = Laboratory determination e=1.76 n=0.64 15 = Laboratory determination welding 80 kPa	

Data sheet compiled in situ for the deposit of Pozzolanelle

SITE: CAVA IMETER- ROMA OPERATOR: GEOL. M. SCARAPAZZI DATE: 22/02/08	
1. STATION: Nord side, 2. LAYER: A (Congl. giallo), 3. THICKNESS: ~2 m, 4. ORIENTATION: Horizontal	
5. PYROCLASTIC TYPE <input checked="" type="checkbox"/> Lithoid <input type="checkbox"/> Welded <input type="checkbox"/> Granular <input type="checkbox"/> Altered <input type="checkbox"/> Deeply altered	
6. COLOUR Matrix: dry light yellowish-brown (Munsell cod 10 YR 6/4) wet brown (Munsell cod 10 YR 4/3) Clasts: dry varius colors grey, light pinkish-brown, black, ecc. wet varius colors grey, pinkish-brown, black, ecc.	
7. SEDIMENTARY STRUCTURE <input type="checkbox"/> Stratified <input type="checkbox"/> Graded <input type="checkbox"/> Laminated <input checked="" type="checkbox"/> Massive <input checked="" type="checkbox"/> Homogeneous <input type="checkbox"/> Not homogeneous	
8. CLAST NATURE <input type="checkbox"/> 80% Juvenile <input type="checkbox"/> 50% Matrix <input type="checkbox"/> >15% Secondary <input type="checkbox"/> 30% Clasts <input type="checkbox"/> 20% Scoria <input type="checkbox"/> 5% Pumices <input type="checkbox"/> 5% Crystals <input type="checkbox"/> < 5% Other (accidental sedimentary/ xenoliths / sedimentary)	
9. TEXTURE <input type="checkbox"/> Granular sustained <input type="checkbox"/> Intermediate <input checked="" type="checkbox"/> Matrix sustained	
10. CLAST ORIENTATION <input checked="" type="checkbox"/> Isotropic <input type="checkbox"/> Anisotropic <input type="checkbox"/> Imbricated (Attitude)	
11. GRADING Blocks / Bombs (d > 2mm) 0% Lapillus (2 - 4mm) 30% Coarse ash (0.063 - 2 mm) 35% Medium to Fine ash (< 0.063 mm) 35%	
12. ANGULARITY <input type="checkbox"/> Very angular <input type="checkbox"/> Angular <input checked="" type="checkbox"/> Subangular <input type="checkbox"/> Subrounded <input type="checkbox"/> Rounded <input type="checkbox"/> Very rounded	
13. VESICULATION <input type="checkbox"/> High <input type="checkbox"/> Medium <input checked="" type="checkbox"/> Low <input type="checkbox"/> Absent	
14. POROSITY <input type="checkbox"/> High <input checked="" type="checkbox"/> Medium <input checked="" type="checkbox"/> Low	
15. BONDING <input checked="" type="checkbox"/> True <input type="checkbox"/> Electrostatic <input type="checkbox"/> Apparent <input checked="" type="checkbox"/> Welding <input type="checkbox"/> Low <input type="checkbox"/> Absent <input type="checkbox"/> Medium <input checked="" type="checkbox"/> High	
NOTES: 2 = Single Level; 8 = Determination made by visual analysis, are recognizable minerals of leucite. 11 = Granulometry determined by sieving and sedimentation analysis. 14 = Laboratory determination e=0.41 n=0.29	

Data sheet compiled in situ for the deposit of Conglomerato Giallo

Appendix

SITE: CAVA TACETER - ROMA OPERATOR: GEOL. M. SCARAPAZZI DATE: 22/02/08	
1. STATION: N. side 2. LAYER: B (Pozz. Nera) 3. THICKNESS: 18 m 4. ORIENTATION: Horizontal	
5. PYROCLASTIC TYPE <input type="checkbox"/> Lithoid <input checked="" type="checkbox"/> Welded <input type="checkbox"/> Granular <input type="checkbox"/> Altered <input type="checkbox"/> Deeply altered	
6. COLOUR Matrix: dry greenish-grey (Munsell: Gley 1 5/2) wet dark greenish-grey (Munsell: Gley 1 4/1) Clasts: dry light grey (Munsell: Gley 1 6/1) wet light grey (Munsell: Gley 1 6/1)	
7. SEDIMENTARY STRUCTURE <input type="checkbox"/> Stratified <input type="checkbox"/> Graded <input type="checkbox"/> Laminated <input checked="" type="checkbox"/> Massive <input checked="" type="checkbox"/> Homogeneous <input type="checkbox"/> Not homogeneous	
8. CLAST NATURE Juvenile: >95% Secondary: <2% Other (accidental sedimentary xenolites / sedimentary): none% Matrix: 60% Clasts: 35% Scoria: 0% Pumices: 0% Crystals: 5%	
9. TEXTURE <input type="checkbox"/> Granular sustained <input checked="" type="checkbox"/> Intermediate <input type="checkbox"/> Matrix sustained	
10. CLAST ORIENTATION <input checked="" type="checkbox"/> Isotropic <input type="checkbox"/> Anisotropic <input type="checkbox"/> Imbricated	
11. GRADING Blocks / Bombs: 0% Lapilli: >50% Coarse ash (125-250 μm): 30% Medium to Fine ash (10-125 μm): <20%	
12. ANGULARITY <input type="checkbox"/> Very angular <input checked="" type="checkbox"/> Angular <input checked="" type="checkbox"/> Subangular <input type="checkbox"/> Subrounded <input type="checkbox"/> Rounded <input type="checkbox"/> Very rounded	
13. VESICULATION <input type="checkbox"/> High <input type="checkbox"/> Medium <input checked="" type="checkbox"/> Low <input checked="" type="checkbox"/> Absent	
14. POROSITY <input type="checkbox"/> High <input checked="" type="checkbox"/> Medium <input checked="" type="checkbox"/> Low	
15. BONDING <input checked="" type="checkbox"/> True <input type="checkbox"/> Electrostatic <input checked="" type="checkbox"/> Apparent <input checked="" type="checkbox"/> Welding <input type="checkbox"/> Low <input checked="" type="checkbox"/> Medium <input checked="" type="checkbox"/> High <input type="checkbox"/> Absent	
NOTES: 2 = Single Level; 6 = Determination made by visual analysis, are recognizable minerals of fucite. 11 = Granulometry determined by sieving and sedimentation analysis. 14 = Laboratory determination: n=030 n=045 15 = Laboratory determination: 300 MPa	

Data sheet compiled in situ for the deposit of Pozzolana Nera

References

Alberti A, Dragone M, Manfredini M, Segre AG (1967) Carta Geologica d'Italia, Foglio 150 Roma, scala 1:100000, 2nd edn. Sev. Geolog. It

Barton NR, Choubey V (1977) The shear strength of rock joints in theory and practice. *Rock Mech* 10:1-54

Bernabini M, Esu F, Martinetti S, Ribacchi R (1966) On the stability of the pillars in an underground quarry worked through soft pyroclastic rocks. *Proc I Congr Int Soc Rock Mech*, Lisboa

Camponeschi B, De Casa G, Giglio G, Volponi E (1982) Studio geologico-tettonico delle tavolette Ardea e Torre S. Lorenzo. Foglio 158 della Carta d'Italia, pp 151-180

CARG (1992) La geologia di Roma dal centro storico alla periferia. In: Funicello R, Praturlon A, Giordano G (eds) APAT. Memorie descrittive della carta geologica d'Italia

Cattoni E (2003) Comportamento meccanico e proprietà idrauliche della Pozzolana Nera dell'area romana in condizioni di parziale saturazione. Ph.D. Thesis, Università di Perugia

Cattoni E, Cecconi M, Pane V (2007) Geotechnical properties of an unsaturated pyroclastic soil from Roma. *Bull Eng Geol Environ* 66:403-414

Cecconi M (1998) Sample preparation of a problematic pyroclastic rock. *Proc IS Probl Soils Sendai* 1:165-168

Cecconi M (1999) Caratteristiche strutturali e proprietà meccaniche di una piroclastite: la Pozzolana Nera dell'area romana. Ph.D. Thesis, Università di Roma Tor Vergata

Cecconi M, Viggiani GMB (1998) Physical and structural properties of a pyroclastic soft rock. *Proc II Int Symp Hard Soils/Soft Rocks Napoli* 1:85-91

Cecconi M, Viggiani GMB (2000) Stability of sub-vertical cuts in pyroclastic deposits. In: *Geoen 2000 international conference on geotechnical & geological engineering*, Melbourne, Australia, on CD rom

Cecconi M, Viggiani GMB (2001) Structural features and mechanical behaviour of a pyroclastic weak rock. *Int J Numer Anal Meth Geomech* 25:1525-1557

Cecconi M, Viggiani GMB, De Simone A, Tamagnini C (2003) A coarse grained weak rock with crushable grains: the Pozzolana Nera from Roma, International Workshop on "Constitutive Modelling and Analysis of Boundary Value Problems in Geotechnical Engineering—3X4", Napoli 22-24 Aprile 2003, Hevelius Edizioni, pp 157-216

Cecconi M, Evangelista A, Nicotera MV, Pane V, Cattoni E, Scotto di Santolo A (2005) Wetting paths upon shearing: experimental evidence and comparative analysis of two volcanic soils in the area of Napoli and Roma. In: Trento A, Romero EJ, Cui YJ (eds) *Int. symp. on advanced experimental unsaturated soil mechanics*, Balkema

Croce A (1954) Sulla compressibilità delle pozzolane quali terreni di fondazione. *Geotecnica*

Croce A, Penta F, Esu F (1961) Engineering properties of volcanic soils. V ICSMFE, Paris

De Rita D, Funicello R, Rosa C (1988) Caratteristiche deposizionali della II colata piroclastica del tuscolano-Artemisio. *Boll GNV*

De Rita D, Faccenna C, Funicello R, Rosa C (1995) Stratigraphy and volcano-tectonics. In: Trigila (ed) *The volcano of the Alban Hills*, Tipografia SGS Roma

De Rita D, Fabbri M, Giordano G, Rodani S (2000) Proposta di organizzazione della stratigrafia delle aree vulcaniche secondo i principi delle unità stratigrafiche a limiti inconformi e sua informatizzazione. *Bollettino Della Società Geologica Italiana* 119:749-760

De Rita D, Giordano G, Esposito A, Fabbri M, Rodani S (2002) Large volume phreatomagmatic ignimbrites from Colli Albani Volcano (Middle pleistocene, Italy). *J Volcanol Geoth Res* 118:79-98

Del Prete M, Guadagno FM, Hawkins AB (1998) Preliminary report on the landslides of 5 May 1998, Campania, southern Italy. *Bull Eng Geol Env* 57:113-129

Diano G (2005) Caratterizzazione geomeccanica di Unità eruttive del distretto vulcanico dei Colli Albani (Lazio Centrale). Ph.D. Thesis, Università di Roma La Sapienza

Esposito L, Guadagno FM (1998) Some special geotechnical properties of pumice deposits. *Bull Eng Geol Env* 57:41-50

Evangelista A, Aversa S (1994) Experimental evidence of non-linear and creep behaviour of pyroclastic rocks. In: Udine, Cristescu, Gioda (eds) *Viscoplastic behaviour of geomaterials*, CISM Courses and Lectures, n. 350. Springer, pp 55-101

Ferrara G, Laurenzi MA, Taylor HP Jr, Taroni S, Turi B (1985) Oxygen and strontium isotope studies of K-rich volcanic rocks from the Alban Hills, Italy. *Earth Planet Sci Lett* 75:13-28

Fisher RV, Schmincke HU (1984) *Pyroclastic rocks*. Springer, Berlin

Fornaseri M, Scherillo A, Ventriglia U (1963) *La regione vulcanica dei Colli Albani*. Consiglio Nazionale delle Ricerche, Roma

Freda C, Gaeta M, Palladino DM, Trigila R (1997) The Villa Senni (Alban Hills, central Italy): the role of H₂O and CO₂ on the magma chamber evolution and on the eruptive scenario. *J Volcanol Geotherm Res* 78:103-120

Funicello R, Giordano G, De Rita D (2003) The Albano Maar lake (Colli Albani Volcano, Italy): recent volcanic activity and evidence of pre-Roman Age catastrophic lahar events. *J Volcanol Geoth Res* 123:43-61

Gaeta M, Freda C, Christensen JN, Dallai L, Marra F, Karner DB, Scarlato P (2006) Time-dependent geochemistry of clinopyroxene from the Alban Hills (Central Italy): clues to the source and evolution of ultrapotassic magmas. *Lithos* 86:330-346

- Gagliardi C (2002) Comportamento meccanico di un materiale granulare a grani frantumabili. Tesi di laurea. Università di Roma Tor Vergata
- Gillespie MR, Styles MT (1999) Classification of igneous rocks. British Geological Survey Research Report RR 99–06. BGS Rock Classification Scheme, vol 1
- Giordano G, De Benedetti AA, Diana A, Diano G, Gaudio F, Marasco F, Miceli M, Mollo S, Cas RAF, Funicello R (2006) The Colli Albani mafic caldera (Roma, Italy): stratigraphy, structure and petrology. *J Volcanol Geotherm Res Elsevier* 155:49–80
- Goodman RE (1989) Introduction to rock mechanics. Wiley, New York
- Hoek E (1968) Brittle failure of rock. In: Stagg KG, Zienkiewicz OC (eds) *Rock mechanics in engineering practice*. Wiley, London, pp 99–124
- Hoek E, Brown ET (1980) Empirical strength criterion for rock masses. *J Geotech Eng Div ASCE* 106(GT9):1013–1035
- Hoek E, Carranza-Torres C, Corkum B (2002) Hoek-Brown failure criterion. In: *Proceedings of 5th North American rock mechanics symposium*, Toronto, Canada, pp 267–273
- Houghton BF, Wilson CJN (1989) A vesicularity index for pyroclastic deposits. *Bull Volcanol* 51(6):451–462
- Karner DB, Marra F, Renne PR (2001) The history of the Monti Sabatini and Alban Hills volcanoes: groundwork for assessing volcanic-tectonic hazards for Rome. *J Volcanol Geotherm Res* 107(1–3):185–215
- Lee IK (1991) Mechanical behaviour of compacted decomposed granite soil. PhD. Thesis, 1991, City University
- Lembo Fazio A, Ribacchi R (1990) Problemi di stabilità di scarpate e cavità sotterranee in rocce piroclastiche. Terzo ciclo di conferenza di meccanica e ingegneria delle rocce: “Le rocce tenere”, Torino
- Mesri G, Godlewski PM (1977) Time and stress compressibility inter-relationship. *J Geotech Eng Div ASCE* 103(GT5):417–430
- Mesri G, Ullrich CR, Choi YK (1978) The rate of swelling of overconsolidated clays subjected to unloading. *Géotechnique* 28(3):281–307
- Miura K, Maeda K, Furukawa M, Toki S (1997) physical characteristics of sands with different primary properties. *Soil Found* 38(4):159–172
- O’Rourke TD, Crespo E (1988) Geotechnical properties of cemented volcanic soil. *J Geotech Eng* 114(10):1126–1147
- Pellegrino A (1967) Proprietà fisico meccaniche dei terreni vulcanici nel napoletano. VIII Convegno di Geotecnica, Cagliari
- Powers MC (1953) A new roundness scale for sedimentary particles. *J Sediment Petrol* 23:117–119
- Salvador A (1987) Unconformity bounded stratigraphic units. *Geol Soc Am Bull* 98:232–237
- Scandone R, Giacomelli L (1998) *Vulcanologia. Principi fisici e metodi d’indagine*. Liguori Editori, Napoli
- Serri G, Innocenti F, Manetti P, Tonarini S, Ferrara G (1991) Il magmatismo neogenico quaternario dell’area toscano-laziale-umbra: implicazioni sui modelli di evoluzione geodinamica dell’Appennino settentrionale. *Studi Geolog Camerti Vol Spec* 1:429–463
- Shepard FP (1963) *Submarine geology*. Harper & Row, Evanston
- Taylor DW (1948) *Fundamentals of soil mechanics*. Wiley, New York
- Turi B, Taylor, HPJ, Ferrara G (1991) Comparisons of $^{18}\text{O}/^{16}\text{O}$ and $^{87}\text{Sr}/^{86}\text{Sr}$ in volcanic rocks from the Pontine Islands, M. Ernici, and Campania with other areas in Italy. In: Taylor HP, O’Neil JR, Kaplan IR (eds) *Stable isotope geochemistry: a tribute to Samuel Epstein*. *Geoch Soc Spec Paper*, vol 3, pp 307–324
- Trigila R, Agosta E, Currado C, De Benedetti AA, Freda C, Gaeta M, Palladino DM, Rosa C (1995) *Petrology*. In: Trigila R (ed) *The volcano of the Alban Hills*. SGS, Rome, pp 95–165
- Vaughan PR (1988) Characterising the mechanical properties of in situ residual soils. In: *Proceedings of 2nd international conference on geomechanics in tropical soils*, Singapore, pp 469–487